State-of-the-art in microwave processing of metals, metal powders and alloys

Forhad Hossain [a,b], Jeffrey V. Turner [b], Robert Wilson [b], Ling Chen [b], Geoffrey de Looze [b], Samuel W. Kingman [c], Chris Dodds [c], Georgios Dimitrakis [a,*]

[a] George Green Institute for Electromagnetics Research, Faculty of Engineering, University of Nottingham, University Park, Nottingham, NG7 2RD, United Kingdom
[b] CSIRO (Commonwealth Scientific and Industrial Research Organisation) Manufacturing, Advanced Materials and Processes Group, Private Bag 10, Clayton South, Victoria, 3169, Australia
[c] Advanced Materials Research Group, Faculty of Engineering, University of Nottingham, University Park, Nottingham, NG7 2RD, United Kingdom

ARTICLE INFO

ABSTRACT

Discovery of the capacity of microwave energy to heat materials was a major milestone in the history of technology and scientific research. This discovery led to the development of many devices and processes that have replaced conventional heating methods, thereby reducing reliance on fossil fuels and reducing atmospheric CO_2 emissions. Over the past two decades the use of microwave heating for processing of non-dielectric metals, metal powders alloys have increased markedly and includes sintering, melting, joining, cladding, drilling, and 3D printing. These developments have used a wide range of experimental procedures, and the use of microwave power has resulted in significant benefits over conventional heating methods. These benefits include a many-fold decreases in processing times and energy consumption, as well as improved microstructural characteristics and mechanical properties of the processed material. This review provides a comprehensive overview of the state-of-the-art of microwave processing of metals, metal powders and their alloys and focuses on important process parameters such as heating mechanisms, electromagnetic properties of metals, the factors affecting these parameters and applications to metal processing. Requirements for efficient metal processing using microwave power are presented including metal properties, microwave susceptors, insulators, ceramic containment structures and temperature measurement methods that all play roles in the development of microwave processing of metals and metal alloy materials. Current challenges and issues in equipment design parameters and various processing methods to facilitate commercial implementation of metal processing at larger scales are investigated.

Nomenclature

Abbreviations		k	Wave number (m^{-1})
AlN	Aluminium Nitride	H_o	Incident magnetic field (A m^{-1})
AM	Additive manufacturing	ω	Angular frequency (rad s^{-1})
B$_4$C	Boron carbide	ε_o	Vacuum permittivity (F m^{-1})
BN	Boron nitride	ε	Complex permittivity (F m^{-1})
E-field	Electric field	μ	Complex permeability (H m^{-1})
EM	Electromagnetic	μ_0	Vacuum permeability (H m^{-1})

(continued on next column)

(continued)

Abbreviations		k	Wave number (m^{-1})
EIA	Energy Information Administration	ε_r	Dielectric constant
H-field	Magnetic field	σ	Electrical conductivity (S m^{-1})
IEA	International Energy Agency	J	Current density (A m^{-2})
ISM	Industrial, Scientific, and Medical	δ	Skin depth (μm)
MMCs	Metal matrix composites	ρ_e	Material resistivity (Ω m)
MoSi$_2$	Molybdenum disilicide	P_d	Dielectric loss (W m^{-3})
MW	Microwave	ε_d''	Imaginary part of the permittivity (F m^{-1})
MWSCs	Microwave susceptible ceramics	W_H	Joule heating (W m^{-3})
MHH	Microwave hybrid heating	r_c	Radius of particle core (m)

(continued on next page)

---

* Corresponding author.
  E-mail address: georgios.dimitrakis@nottingham.ac.uk (G. Dimitrakis).

(continued)

Abbreviations		k	Wave number (m^{-1})
NW-MWSC	Non-wettable microwave susceptible ceramics	m	Magnetic dipole moment (A m^{-2})
PTFE	Polytetrafluoroethylene	R_s	Surface resistance (ohm)
SPS	Spark plasma sintering	μ_d''	Imaginary part of the permeability
CT	X-ray computed tomography	θ_Y	Contact angle (degree)
TiC	Titanium carbide	R_L	Reflection coefficient
VFM	Variable frequency microwaves	Z_{in}	Impedance of sample (ohm)
YSZ	Yttria-stabilized zirconia	Z_0	Impedance of free space (ohm)
Symbols		d	Sample thickness (m)
F	Microwave frequency (Hz)	$\tan\delta$	Loss factor
A	Particle radius (m)	P_c	Conduction loss (W m^{-3})
C	Velocity of light in vacuum (ms^{-1})	P_E	Electric dipole absorption
λ_o	Free space wavelength (m)	P_H	Magnetic dipole absorption
P	Electric dipole moment (C m)	ρ_s	Material porosity
E_o	Incident electric field (V m^{-1})	μ_r	Relative permeability

1. Introduction

The consumption of global natural resources including materials and energy, has increased considerably in recent years due to ongoing industrial development and almost exponential growth in production and manufacturing. This increasing energy demand has resulted in unsustainable levels of carbon dioxide emission and the generation of large volumes of waste. In comparison to other end-use sectors, according to the International Energy Agency's (IEA) Global Energy Review 2021, the industrial sector had the largest share of global energy consumption that accounted for approximately 38 % of total energy consumption in 2020 [1]. According to the U.S. Energy Information Administration (EIA), the manufacturing sector accounts for over 80 % of industrial energy usage, and the metal production industry together with paper production accounted for almost half (48.8 %) of all energy consumed by the manufacturing sector [2]. In practice, the manufacturing sector employs a wide range of conventional heating technologies, including electric arc furnaces, induction furnaces, blast furnaces, cupola furnaces for processing metals. These conventional heating systems typically have characteristic disadvantages of slow heating rates, prolonged processing times, non-uniform heating, and high energy consumption all of which contribute to CO_2 emissions and environmental pollution. Therefore, there is an significant demand for high performance, faster, eco-friendly, sustainable, and low energy consuming heating and process technologies for a wide range of materials including metals [3]. According to specific needs and applications, one or more advanced heating methods, such as electron beam, plasma heating, microwave heating, magnetic induction, and solar heating have been reported in the literature as alternatives to conventional high-temperature treatment methods [4]. Through the development and application of these advanced and efficient heating technologies global energy consumption can be reduced thereby securing sustainable energy resources for the future [3]. Heating using microwave power is one of these promising sustainable options and is receiving considerably increased attention because of its capacity to address the above challenges.

The range of the electromagnetic (EM) spectrum designated as microwaves spans from 300 MHz to 300 GHz. This frequency range corresponds to wavelengths that increase as the frequency decreases from 1 m to 1 mm, respectively in free space. Most frequency bands in the microwave spectrum are reserved for communication, and only a small number (ISM bands) are permitted for use in industrial heating applications. These are performed most often at the frequencies 915 MHz, 2.45 GHz, 5.8 GHz, and 24.124 GHz [5,6]. Unlike conventional heating, which occurs when energy is transferred from an external source and heat transfer occurs from the surface of the load to the core, microwave
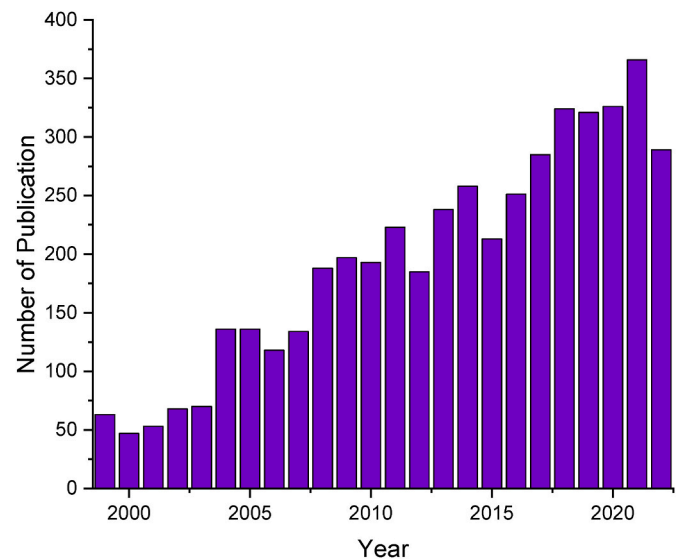

Fig. 1. Number of publications related to microwave processing of metallic materials for the period 1999–2022 (Sources: Scopus and Science Direct).

heating reverses the heating pattern by heating internally before dispersing to the surface [7]. This unique characteristic of microwave heating offers many advantages in material processing due to its penetrating radiation, high-speed heating, volumetric heating, uniform heating, absence of contamination, energy efficiency and sustainable processing [5,8–10]. These characteristics of microwave heating allowing significant process flexibility and the opportunity to customise processes for specific individual metals.

Microwave heating was first introduced in 1999 forming a new paradigm for application to processing of metallic materials [11]. It was demonstrated that microwave power will interact with metal powders or bulk metals generating high temperatures for example microwave power was used successfully to sinter metals [11]. Further investigations were conducted on the heating of different metals under high electric (E) and magnetic (H) microwave fields using single mode applicators [12,13]. It was reported that while magnetic metals heated more effectively when placed within a strong magnetic field, others heated more effectively when placed in regions with stronger electric field [12,13]. Theoretical analysis was presented that demonstrated each material has an optimum powder size for microwave heating, with the maximum absorption determined by the ratio of the mean particle radius to the skin depth [14]. The effects of microwave power on the mechanical and metallurgical characteristics of sintered metal compacts was investigated [9] and when compared the results to those of conventional heating showed that process duration was shortened, densification was enhanced, porosity was reduced, coarsening was reduced, and oxidation was reduced. Based on these advantages microwave energy is finding increasing applications in metal processing including joining similar and dissimilar metals, brazing, melting, cladding, casting, drilling, coating, 3D printing and development of thermoelectric and magnetic materials for waste heat recovery and improving energy recovery. According to Scopus and Science Direct data of the approximately 250 relevant papers scrutinised the overall publishing activity on microwave processing of metallic materials and its alloys is continuously growing, as shown in Fig. 1. The corresponding research trends for major metal applications is shown in Fig. 2. The timeline of when various applications occurred is represented by the year (x-axis), indicating the time of first introduction. The number of publications up to 2022 that specifically focus on each application are shown on the y-axis.

Several comprehensive reviews exist on the microwave processing of materials including polymers, ceramics, and metallic materials and their alloys. These have mainly considered microwave-material interactions
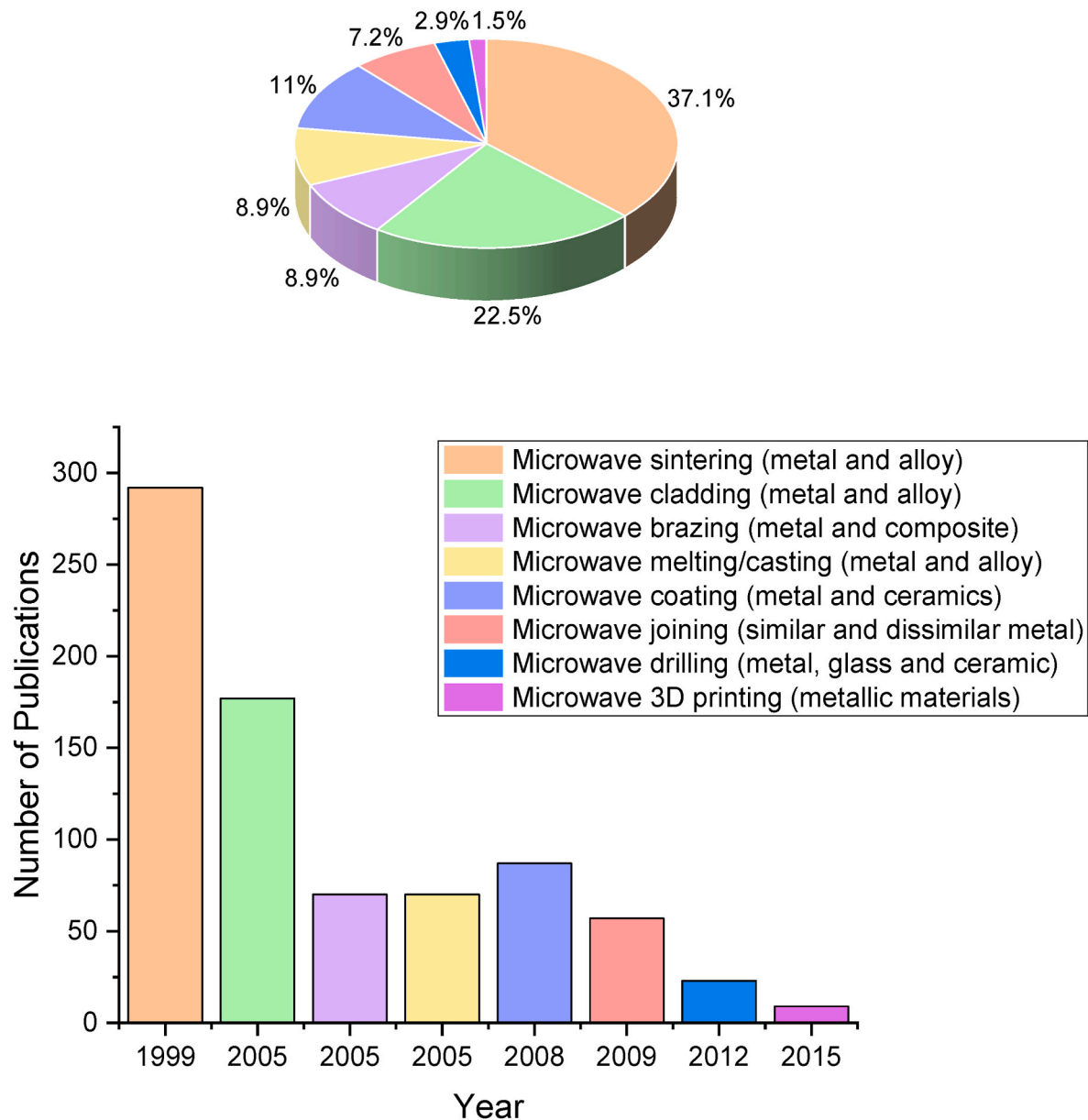
Fig. 2. A timeline of the most important microwave metal processing along with research trends and percentage contributions based on publications until 2022.

and heating phenomena [15–21]. However, there remains an information gap relating to performance enhancement during the use of microwave energy for metal processing. There remains a requirement for further research, particularly in the areas of scaling-up, in-depth evaluations of performance and comparisons between microwave-based metal processing applications and existing methods. By concentrating on these areas, researchers and engineers can advance the knowledge in the field and prepare it for greater commercial adoption. This review aims to present state of the art information on the methodologies of microwave metal processing, system design, implementation, and performance evaluation for cutting-edge applications. Additionally, the review outlines the challenges associated with this technology and offers recommendations for future research directions. It also presents novel design considerations for developing bespoke microwave systems, of possible commercial interest due to low cost (e.g. ~$250 k) entry level bench-top systems such as small-scale gold casting for the jewellery and electronics industries.

The review is structured as follows: Section 1 introduces the background of microwave heating for metal processing; Section 2 microwave

system fundamentals and the theory of microwave interaction with metal particles; Section 3 methodologies and applications of microwave power in processing metal and metal alloys; Section 4 discusses challenges and outlines future development aspect. Finally, Section 5 provides a conclusion summarizing the key findings and insights presented throughout the review.

2. Microwave systems

A microwave system consists of three key components: a microwave generator, a waveguide, and an applicator. The generator produces electromagnetic energy at a given frequency which is then delivered to the applicator via the waveguide. The applicator is a cavity that contains the material to be processed and functions to transfer the microwave energy from the waveguide to the target material or load. Several electronic components, such as magnetrons, klystrons, travelling wave tubes, and solid-state microwave devices can generate microwave power. The applicator's size and shape can be customized to improve power focussing and heating efficiency and it is categorized as either
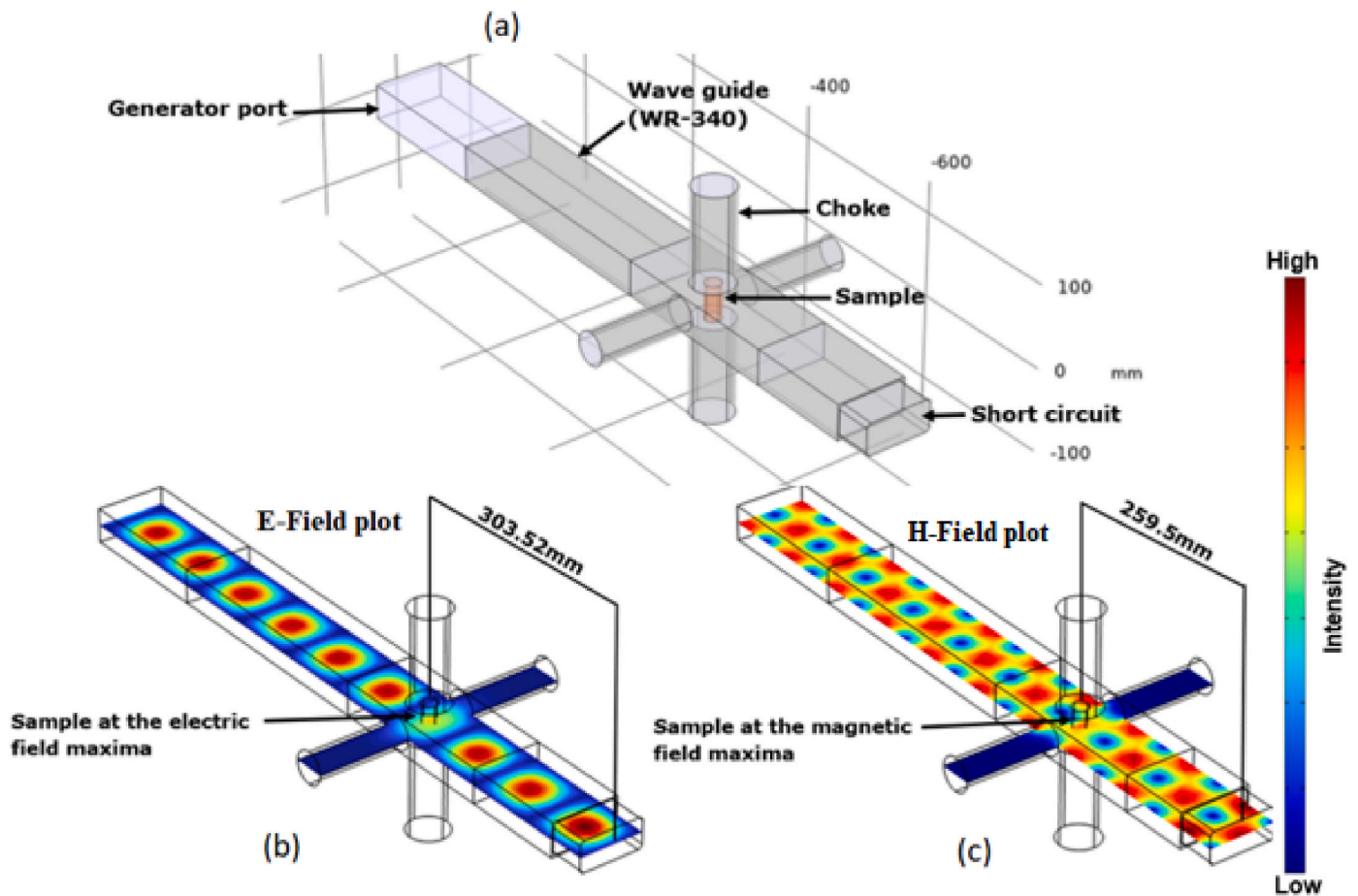
Fig. 3. (a) Single mode waveguide applicator geometry; (b) Electric (E) field distribution; (c) Magnetic (H) field distribution. Source: Authors.

single-mode or multimode. Single-mode applicators have a well-defined electric and magnetic field patterns with high-intensity levels that can be confined to small volumes, making them suitable for heating small load volumes Single-mode applicators can be tuned to focus microwave energy on the load. The precise placement of the load within the applicator is crucial for effectively heating it. Fig. 3 shows a simulation of the electromagnetic field distribution of the electric (E-field) and magnetic (H-field) for a single mode waveguide applicator distribution. At a microwave frequency of 2.45 GHz and wavelength $\lambda_o \sim 122.4$ mm, the distance between the electric (E-field) and magnetic (H-field) field maxima is a quarter of the wavelength $\lambda_o/4 \approx 30.5$ mm. In this configuration, a choke (a small opening of less than $\lambda_o/4$) enables accurate positioning of the load and adjustment of the short circuit position allows for either the E-field or H-field maxima to be aligned precisely at the load point. Multimode applicators are used for larger samples requiring uniform heating. In multimode applicators the cavity dimensions are generally large compared to the operating wavelength, allowing the formation of multiple modes. Microwave interaction phenomena and energy conversion largely depends on material properties and based on how they interact with microwaves, can be divided into three groups: (i) Microwave transparent materials such as glass and many ceramics that have little or no interaction with microwaves at room temperature pass through the materials with little attenuation no energy is converted to heat. Some glasses and ceramics can transform to being microwave absorbent at higher temperatures. (ii) Microwave absorbent materials such as water, foods containing water, and in general materials containing O–H bonds absorb microwave energy and dissipate it into the material as heat. (iii) Materials such as bulk metals are opaque to microwaves and reflect microwaves thus microwave energy does not penetrate into the materials and does not generate heat.

Microwave interaction mechanisms for microwave absorbent materials and ceramics have been investigated extensively, and physics of interaction is now well understood [20,22]. Microwave heating of absorbent materials has been applied to numerous applications, including adaptations for large scale industries. Considerably less effort has been made to understand microwave interaction phenomena for opaque or metallic materials, as the assumption has always been that bulk metals have high electrical conductivity they cannot be heated by microwaves [23]. However, after the publication of a groundbreaking study [11] this field of research began to attract greater attention.

2.1. Microwave interaction mechanisms with metal particles

Microwave energy absorption by metal particles is governed by several factors. Firstly, metals interact with two components of the electromagnetic fields, the electric field (E) and the magnetic field (H). This depends on the microwave operating frequency, the size and shape of the metal particle and the electromagnetic properties of the metal. The extent to which metal particles interact and heat up when subjected to microwave fields also depends on the penetration depth, applicator geometry, the operating mode (single or multi-mode), the position of the load inside the applicator, and the use of susceptors (lossy microwave-absorbing materials).

2.2. Role of the electric field

Metals are highly electrically conductive due to the abundance of free electrons. When the alternating electric field of the microwave is applied, the free electrons move back and forth through the metal's surface in response to the alternating electric field resulting in induced
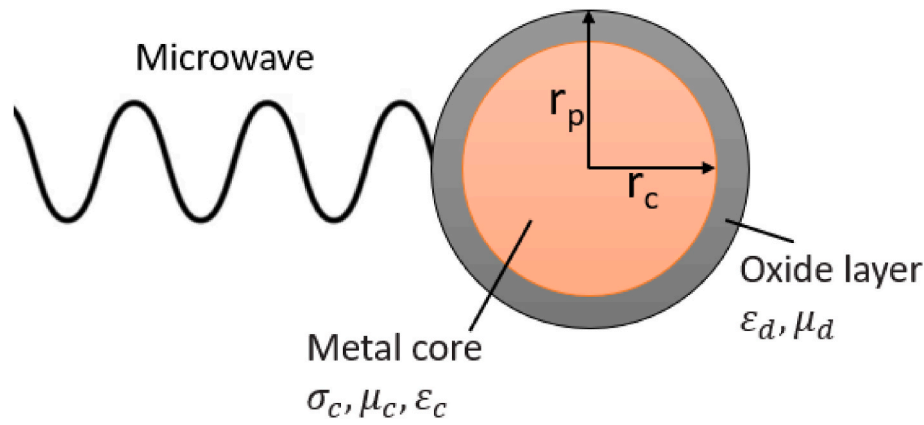
Fig. 4. The interaction of microwaves and metal particles is for illustration purposes. Source: adapted from Ref. [28].

currents. The induced current produces a magnetic field that is opposite to the original field inside the metal particle and repels the conducting electrons outside the metal surface. These electrons build up in the form of energised electron clouds that generate a plasma in the gas atmosphere in contact with the metal. This energy is focused especially along the sharp edges of bulk metals. Therefore, in such a case, bulk metals are not heated by an external microwave electric field (E-field) because the energy is dissipated in the form of a gas plasma [21]. However, metallic powders behave differently when exposed to the microwave E-field and are heated if the particle size is within a certain range. There have been limited efforts to provide theoretical explanations for the interaction between microwaves and powdered metals. Furthermore, the theoretical models described in previous studies are complex, necessitate demanding computation, require assumptions in the calculations and are limited to specific scenario [14,23–26]. This section will consider two theoretical models of microwave E-field interactions with conductive particles. The first model is based on principle of electric dipole absorption and explains how conducting particles can be effectively heated by microwave energy and is applicable to a range of particle sizes and conductivities [14]. Their assumptions include that the conducting particles are spherical, electrically small (particle size $\ll \lambda_0$, the free space wavelength) and that electromagnetic scattering can be neglected. The particle distribution is in a vacuum at a volume filling fraction of less than 0.01, resulting in low permittivity and minimal losses. Due to their uniform size, each particle absorbs energy equally, contributing to the overall absorption. The electric dipole moment p for a conducting sphere with radius a placed in a uniform electric field E_0 was expressed as [14]:

$$\vec{p} = 2\pi a^3 \vec{E}_0 \left[\frac{(2\varepsilon + 1)(1 - ka \cot ka) - (ka^2)}{(\varepsilon - 1)(1 - ka \cot ka) + (ka^2)} \right] \tag{1}$$

Where, $k = \frac{\omega\sqrt{\varepsilon\mu}}{c}$ is the wave number within the particle, c is the speed of light, ω is the angular frequency, $\varepsilon = \varepsilon_1 - j\varepsilon_2$ is the complex permittivity, the real part of the permittivity, $\varepsilon_1 = \varepsilon_r\varepsilon_0$, $\varepsilon_0 = 8.854 \times 10^{-12}$ F/m, ε_r is the dielectric constant, $\varepsilon_2 = \frac{\sigma}{\omega\varepsilon_0}$ is the imaginary part of the permittivity also called the loss factor, σ is the bulk electrical conductivity, $\mu = \mu_1 - j\mu_2$ is the complex permeability of the particles, the real part of the permeability $\mu_1 = \mu_0\mu_r$, μ_r is relative permeability and free space permeability $\mu_0 = 4\pi \times 10^{-7}$ H/m, μ_2 is the magnetic loss factor. The time average power dissipation in the spherical particle is associated with electric dipole absorption and expressed as [14]:

$$\langle P_E \rangle = -\frac{3\omega}{8\pi a^3} Im\left(\vec{p} \cdot \vec{E}_0^*\right) \tag{2}$$

Substituting the value of dipole absorption in Equation (2), the power dissipation is expressed as [14]:

$$\langle P_E \rangle = -\frac{3}{4}\omega\varepsilon_0 E_0^2 Im\left[\frac{(2\varepsilon + 1)(1 - ka \cot ka) - (ka^2)}{(\varepsilon - 1)(1 - ka \cot ka) + (ka^2)}\right] \tag{3}$$

Where, E_0 is the peak value of the applied electric field. Further assuming $\varepsilon_1 = \mu = 1$, $\varepsilon = 1 - j\frac{\sigma}{\omega\varepsilon_0}$ for a range of conductivity. The power dissipation Equation (3) behaves differently depending on how the particle radius, a compared to the skin depth, δ. The skin depth also termed the penetration depth is the distance from the materials surface into the interior at which the magnitude of field strength decreases by a factor $1/e \sim 0.368$. The penetration depth of a material can be calculated using following equation [27]:

$$\delta = \frac{1}{\sqrt{\pi f \mu \sigma}} = 0.029(\rho_e \lambda_0)^{0.5} \tag{4}$$

Where, ρ_e is the conductor resistivity(Ωm). If the skin depth is much larger than the radius of the particle (i.e. $\frac{a}{\delta} \ll 1$) Equation (3) reduces to the quasi-static result, the power dissipation is independent of particle radius and influenced solely by the bulk properties of the material rather than its size as in Equation (5) [14].

$$\lim_{a/\delta \to 0} \langle P_E \rangle = -\frac{3}{2}\omega\varepsilon_0 E_0^2 Im\left(\frac{\varepsilon - 1}{\varepsilon + 2}\right) \tag{5}$$

Now, depending on the conductivity, the power dissipation will change. When $\varepsilon_2 = \frac{\sigma}{\omega\varepsilon_0} \ll 1$ then the power dissipation $\langle P_E \rangle = 9\sigma E_0^2/2$ i.e. the power dissipation is proportional to the conductivity and increases for highly conductive particles. When $\varepsilon_2 = \frac{\sigma}{\omega\varepsilon_0} \gg 1$ then $\langle P_E \rangle = 9\omega^2\varepsilon_0^2 E_0^2/2\sigma$ i.e. power dissipation is inversely proportional to the conductivity. The maximum value of power dissipation is obtained when $\sigma = 3\omega\varepsilon_0$ [14],

$$\langle P_E \rangle_{max} = 3\omega\varepsilon_0 E_0^2/4 \tag{6}$$

In fact, being highly conductive, metallic materials have very small penetration depth (i.e. $\frac{a}{\delta} \gg 1$) and very high conduction loss factor *i.e.* $\varepsilon_2 = \frac{\sigma}{\omega\varepsilon_0} \gg 1$, for such scenario the power dissipation is expressed as [14]:

$$\lim_{a/\delta \to \infty} \langle P_E \rangle = \frac{9\omega^2\varepsilon_0^2 a E_0^2}{4\sigma\delta} \propto a\sqrt{\frac{\omega^5}{\sigma}} \tag{7}$$

Based on the equations, it is understood that the electric dipole absorption increases for larger and weakly to medium conducting particles and reaches its maximum when $\sigma \approx \omega\varepsilon_0$. However, with an increase in conductivity ($\sigma > \omega\varepsilon_0$) the electric field is screened or reflected from the conducting surface, reducing power absorption.

The second model [28] adapted and modified previous theory [25,29,30] to clarify how the metal powder interacts with and absorbs

microwave energy. This modified approach aimed to clarify how the metal powder interacts with and absorbs microwave energy. Their' model's accuracy was confirmed through both numerical simulations and experimental results. The model assumes all the metal particle are spherical and the surface possess a thin layer of oxide. The thickness of the oxide layer or dielectric shell can range from a few nm to μm. The electromagnetic characteristics (σ, ε, μ) of metals as a homogenous solid can change significantly due to the thickness of the oxide layer around the conducting powder particles. The model also assumes a uniform distribution of the microwave field over the particle's surface. The effective medium approximation theory is used to calculate the effective electromagnetic characteristics, with the power dissipation due to the E-field for the sample volume calculated using the following equation [28]:

$$P_d = \omega \varepsilon_0 \varepsilon_d'' (1 - \rho_s) \left[1 - \left(\frac{r_c}{r_p} \right)^3 \right] \int \left| \overrightarrow{E} \right|^2 dV \tag{8}$$

Where ε_d'' is the imaginary part of the relative permittivity of the oxide layer, ρ_s sample's porosity, r_p and r_c are the radius of the whole particle and core respectively as illustrated in Fig. 4.

Equation (8) demonstrates that power dissipation in metal particles is more sensitive to particle size when the radius of the particles is comparable to the thickness of the oxide layer and the imaginary part of the permittivity is high. When the particle size is close to that the thickness of the oxide layer, the maximum power loss occurs, and the sample experiences the fastest heating in the microwave E-field. As the particle size and sample porosity increases power dissipation decreases. Furthermore, as r_c approaches r_p the ratio (r_c/ r_p) tends towards 1, indicating negligible power dissipation. Consequently, without a dielectric layer on the metal particle's surface, there's no power dissipation or heat generation, noting limitation of this model.

2.3. Role of the magnetic field

In order to understand the mechanism of metal-microwave interaction and to distinguish between different heating behaviours, a number of studies have been published outlining experimental results and numerical calculations in separate E− and H-fields [12,26,31–33]. The first experimental proof of different E− and H-field responses was provided when a variety of magnetic and non-magnetic metal powders, ceramics, and metal-ceramic composites were heated using separate electric and magnetic fields [12]. It has been observed that metal powders (e.g. Cu, W, Fe, Co) absorb significant microwave energy in the H-field and temperatures increase far more rapidly than in an electric field [12,13,34]. Subsequent studies reported and verified comparable findings and observations [35–45]. These experimental findings demonstrated that magnetic loss makes a considerable contribution and plays a major role in microwave heating of metals.

Theoretical studies exploring the magnetic loss mechanism have shown several research that might be responsible for temperature increase in metal powders [23,46–49]. The basic mechanisms for H-field heating include hysteresis, eddy currents, magnetic resonance and domain wall oscillations. Two theoretical models of electromagnetic absorption by metal powder in the H-field were proposed. The first model [14] calculated power absorption considering spherical conducting particles of equal radius (a), electrically small particles (particle size ≪λₒ, free space wavelength) and neglected electromagnetic scattering. Considering the particles are placed inside a cavity resonator at maximum magnetic field magnitudes or at the antinodes, for applied magnetic field H_0, the conducing particle will develop a magnetic dipole moment m (m needs a superscripted arrow) expressed as [14]:

$$\overrightarrow{m} = 2\pi a^3 \overrightarrow{H_0} \left[\frac{(\mu + 2)(1 - ka \cot ka) - \mu(ka)^2}{(\mu - 1)(1 - ka \cot ka) - \mu(ka)^2} \right] \tag{9}$$

Where, k is the wavenumber as in Equation (1), μ is the complex permeability. Then the time-averaged power caused by magnetic dipole absorption per unit volume for the sphere can be calculated as follows [14].

$$\langle P_m \rangle = \frac{3\omega\mu_0}{8\pi a^3} Im\left(\overrightarrow{m}.\overrightarrow{H_0} \right) \tag{10}$$

$$\langle P_m \rangle = \frac{3}{4} \omega\mu_0 H_0^2 Im\left[\frac{(\mu + 2)(1 - ka \cot ka) - \mu(ka)^2}{(\mu - 1)(1 - ka \cot ka) - \mu(ka)^2} \right] \tag{11}$$

Where again ω is the angular frequency and H_0 is the peak value of the magnetic field. For nonmagnetic($\mu_r = 1$) conducting particles Equation (7) can be reduced to [14].

$$\langle P_M \rangle = \frac{3}{4} \omega\mu_0 H_0^2 Im\left[1 + \frac{3 \cot ka}{ka} - \frac{3}{(ka)^2} \right] \tag{12}$$

A large skin-depth limit (a/δ≪1) results in Equation (8) reducing to [14].

$$\lim_{a/\delta \to 0} \langle Pm \rangle = \frac{\omega^2 \mu_0^2 a^2 \sigma}{20} H_0^2 \propto \omega^2 a^2 \sigma \tag{13}$$

In the case where the skin depth limit is small (a/δ≫1) Equation (8) reduces to [14].

$$\lim_{a/\delta \to \infty} \langle Pm \rangle = \frac{9R_s}{4a} H_0^2 \propto \frac{1}{a} \sqrt{\frac{\omega}{\sigma}} \tag{14}$$

Where R_s is the surface resistance of the conducting particle and can be calculated $R_s = \sqrt{\frac{\omega\mu_0}{2\sigma}}$ ....

$$\tag{15}$$

Based on the provided equations, it is evident that particles with sizes close to the skin depth experience increased energy absorption, reaching maximum absorption at approximately 2.41 δ. Conversely, when particle size significantly exceeds the skin depth, the rate of power dissipation diminishes.

If conductive particles have magnetic properties, the magnetic dipole absorption can be considerably improved. Introducing magnetic loss $\mu = \mu_1 - j\mu_2$ in conductive particles, the magnetic dipole absorption can be modified to following equation.

$$\lim_{a/\delta \to 0} \langle P_M \rangle = \frac{3}{4} \omega\mu_0 H_0^2 Im\left(\frac{\mu - 1}{2\mu + 1} \right) \approx \frac{9\omega\mu_2\mu_0 H_0^2}{2(2\mu_1 + 1)^2} \tag{16}$$

The approximation shows that, when the particle radius is small compared to the skin depth, a small value for magnetic loss significantly increases the magnetic absorption. From the calculation it becomes evident that both electric and magnetic dipole absorptions exhibit maximum values under specific conditions, particularly related to particle size and conductivity. The maximum electric dipole absorption occurs as described in Equation (6) under a fixed conductivity value $\sigma = 3\omega\varepsilon_0$. This value is practically low at microwave frequencies of 2.45 GHz and practically not effective in heating conductive particles. However, the magnetic field, particularly through magnetic dipole absorption, appears to play a dominant role in heating conductive particles allowing adjustments in both particle radius and conductivity to achieve optimal absorption conditions ($a \approx 2.41\delta$) as described by Equations (13) and (16).

As previously discussed, the second model considered conductive powder particles enclosed by an oxide layer effectively isolating individual metal particles from one another. This condition allows microwaves to penetrate the sample, ensuring that each metal core interacts with the microwave field. Microwave interaction induces surface

currents, commonly referred to as eddy currents, on the metal cores through magnetic induction. This phenomenon facilitates the calculation of power dissipation by leveraging these induced currents [28]. In this model, the following assumption were made (i) all particles are spherical, (ii) the microwave field is assumed to distribute uniformly within a unit volume, (iii) the oxide layers are assumed to be very thin and their thickness increases linearly with temperature.

When the sample is place in uniform magnetic field, the power dissipated in the sample is calculated as

$$P_c = \frac{3(1-\rho_s)r_c^2}{2r_p^3} \sqrt{\frac{\omega\mu_0\mu_c}{2\sigma_c}} \left(1 - e^{-2\alpha_c r_c}\right) \int \left|\vec{H}\right|^2 dV \qquad (17)$$

Where ρ_s is the porosity of sample, r_p and r_c are the radius of the whole particle and core respectively, μ_c and σ_c are the permeability and permittivity of the particle core, $\alpha_c = 1/\delta$ is the attenuation constant of the metal core. Based on Equation (17) the power dissipation increases with decrease in particle size and *vice versa*. Again, as r_c approaches to skin depth higher power dissipation occurs due to increased interaction with the H-field. The particles will tend to dissipate more power as the frequency increases.

An additional dissipative factor called "magnetic loss" was introduced [33] that arises when conductive particles possess magnetic attributes and exposed to a microwave H-field. When subjected to the H-field, the particles' intrinsic magnetic characteristics cause them to swiftly adjust or align with the alternating magnetic field orientation. This rapid adjustment or realignment of magnetic dipoles results in internal friction within the material, transforming the microwave power into heat. The magnetic loss can be expressed as

$$P_d = \omega\mu_0\mu_d''(1-\rho_s)\left[1 - \left(\frac{r_c}{r_p}\right)^3\right] \int_V |H|^2 dV \qquad (18)$$

Therefore, the combined effect of the magnetic H-field on the magnetically conductive particles is

$$P_t = P_c + P_d \qquad (19)$$

Where μ_d'' is the imaginary part of the relative permeability of the oxide layer, ρ_s is the sample porosity, r_p and r_c are the radius of the whole particle and core respectively. The calculations show that the magnetic loss contribution to power loss in a microwave H-field will be at its maximum when the metal core size is small compared to the thickness of the oxide layer. It is also evident that, microwave H-field is more efficient than the E-field for heating metal particles with magnetic properties.

Experimental tests [28] were carried out and compared with simulation results from the mathematical model to evaluate the heating characteristics of Cu powder mixture combined with Al_2O_3 as a core-shell composite using a 2.45 GHz, 1.5 kW single-mode WR340 microwave system. While the simulated heating patterns closely matched the experimental findings, there were some discrepancies attributed to the model's inherent assumptions and limitations. These limitations included factors such as overlooking the heating effects from phase transitions and not fully addressing the complexities associated with mixed powders, including the ability to forecast variations in heating performance among distinct particles with different electromagnetic properties within the mixture.

2.4. Heat generation and thermal behaviour

There are essentially two different heat-generating mechanisms involved when metal powder interacts with microwave power: conduction and plasma formation. Conduction loss is the dominant heating mechanism for highly conductive metal particles [4]. The conduction heat, essentially the Joule losses, are caused by currents propagating

through the metallic conductor. The amount of heat generated over a given time is proportional to the square of the electric current times the conductor resistance. There are several mechanism that can result in Joule loss in metal particles [46]. For instance, when metal particles interact with microwave fields the oscillating magnetic field creates an electromotive force that causes charge carriers to move in response to the force, resulting in a current flow known as eddy current. The induced eddy current itself generates a magnetic field that opposes the change in the magnetic field that created it. The induced current causes Joule heating in the metal particle and limits the increase in the total field within the metal particles [21]. Another contribution to the Joule loss in conduction heating is the magnetization and hysteresis of the magnetic metal particles. In fact, magnetic hysteresis loss heating is rapid and the amount of heat that is generated as a result is proportional to the dimension of the magnetic hysteresis loop. However, the hysteresis effect disappears above the Curie point (the temperature at which a material loses its magnetic characteristics and becomes non-magnetic). Contact with the load domain walls, electron spin resonance, and magnetic anisotropy all contribute to conduction losses that cause metal particles to heat up when they interact with a microwave field [20,48, 50]. The heat generation mechanism through conduction loss has been used in various metal processing applications, such as sintering, melting, and casting, cladding and coating.

Observation suggests that microwaves interacting with metal particles causes plasma formation in gas-filled interstitial spaces which accelerates heat transport at the particle's contact areas thereby enhancing diffusion. During microwave heating, a sharp increase in the sample's temperature has been observed [51–57] which has been attributed to the creation of plasma or an electric discharge. In order to understand the mechanism of plasma formation, it is necessary to define electric discharge and plasma precisely. An electric discharge, or arcing, is a very rapid discharge of electricity caused by a strong electric field that generates an ionised, electrically conducting channel through an insulating medium such as air or an enveloping gas. Arcing results in the emission of light and an acoustic snap when the applied electric field is greater than the insulating medium's dielectric breakdown strength (the breakdown strength of air is ~30 kV/cm) [57]. Repeated electric discharges generate a localised high-temperature region that ionizes gases in the interstitial spaces between the particles. The ionised gas is known as plasma, one of the four states of matter and can achieve a temperature of the order of 7000 °C for very short periods of time [58]. Hence, when microwaves interact with metal powder, it is in the interstitial spaces between the particles containing non-conducting gases where the plasma is produced. When the sample is subjected to the maximum E-field or maximum H-field, the strong electric field generated within the insulating gaseous media occupying the interstitial spaces changes rapidly from a non-conducting to a conducting state. During the rapid transition of electrical discharges local hotspots or micro plasmas are formed and high temperature zones are produced in the metal particles. The high temperatures produced by the concentrated plasma is critical to the heating process and has been employed in various metal processing applications such as drilling, sintering, brazing and additive manufacturing [21,30,59–61].

2.5. The role of particle size and shape

The size distribution of metal particles is extremely important and plays a crucial role as the primary microwave absorber in metal processing using microwave energy. Finer particles absorb microwave energy more efficiently than coarser particles. This leads to rapid and more uniform heating in finer particles, contributing to improved properties in the processed material [62]. Furthermore, the energy absorbed per unit volume of the sample load is dependent on its particle size, and as the particle size decreases from micron to nanometre range the increase in surface area leads to increase in microwave absorption capacity of a compacted metal powder sample [53,55]. The particle radius to skin

depth ratio is in fact more significant for conductive materials than just particle size alone [55]. Microwave energy absorption by nonmagnetic metal spherical particles shape was examined [24] and the Mie solution [46,63] was applied to explain how conductive spherical particles interact and to analyse the heating process of single metal particles when exposed to microwave power. At a microwave frequency of 2.45 GHz, the wavelength $\lambda_o \sim 122.4$ mm, the distance between the electric (E-field) and magnetic (H-field) field maxima is a quarter of the wavelength $\lambda_o/4 \approx 30.5$ mm. This setup allows for precise positioning of small samples at either the E− or H-field maxima. When employing the Mie expression for a conductive particle like copper with the parameter $\sigma = 5.8 \times 10^7$ placed in the E-field maxima, the absorbed power is minimal. This is because the external field induces a surface charge, leading to the generation of a secondary field directed opposite to the original field inside the particle. In materials with high conductivity, like copper, the combined effect of the primary and secondary fields is practically insignificant [46]. However, when the particle is positioned at the H-field maxima, the maximum power dissipation occurs because the alternating incident magnetic field induces a current in the particle. The induced current results in the generation of Joule heat within the particle and is expressed as [46]:

$$W_H = \frac{3\pi}{2}\mu_0 a\delta^2 \omega \left[\frac{a}{\delta}\frac{\sinh\left(\frac{2a}{\delta}\right) + \sin\left(\frac{2a}{\delta}\right)}{\cosh\left(\frac{2a}{\delta}\right) - \cos\left(\frac{2a}{\delta}\right)} - 1\right] H^2 \quad (20)$$

Where a is the radius of the particle, H = 2H$_0$ is the amplitude of the magnetic field and δ is the skin depth. The calculation revealed that microwave absorption is highly influenced by the size of the particle, specifically the a/δ ratio, and there is a theoretical peak at the ratio of 2.4. In situations where $a \gg \delta$, the equation can be simplified to Ref. [46]:

$$W_H = \frac{3\pi}{2}\mu_0 a^2 \delta \omega H^2 \quad (21)$$

From Equation (21), the power dissipation is directly proportional to $a^2\delta$. This heating behaviour exhibits surface characteristics, indicating that heat is generated mostly by the outer layer and subsequently conducted from the outer layer to the core region of the particles. If the particle size is smaller than the skin depth ($a \ll \delta$), the equation is simplified to Ref. [46]:

$$W_H = \frac{2\pi}{15}\mu_0 a^3 \omega \left(a/\delta H\right)^2 \quad (22)$$

In this case, the power dissipation is proportional to $\left(a/\delta\right)^2$ indicating a volumetric behaviour in heating. As the a/δ ratio decreases, the particle's heating becomes more uniform, leading to an accelerated heating rate. Numerical analysis was used to show that particles with sizes close to the skin depth experience increased energy absorption, reaching maximum absorption at approximately 2.41δ [14]. Conversely, when particle size significantly exceeds the skin depth, the rate of power dissipation diminishes [14]. As particle size become considerably larger than the skin depth most of the microwave energy will be reflected and the powder does not heat. Microwave heating experiments were conducted on different grade stainless steel with various particle sizes ranging from 3 μm to 150 μm [64]. The experimental findings revealed that the maximum heating occurred when the particle size was at approximately 2.5 times the skin depth. The size dependent characteristics of microwave heating for nickel powder showed enhanced heating efficiency within the range of 45–150 μm [65]. Larger particles did not heat as much due to increased heat losses, indicating the importance of particle size in optimizing microwave heating processes.

The shape of the metal particle, surface structure, and edges have all been shown to influence microwave absorption by metal particles.

Table 1

Examples of selected metals that have been processed with microwave power, including their conductivity, penetration depth, and magnetic affinity [30, 70–72].

Metals	Conductivity, σ (Ωm)$^{-1}$ at 20^0 C	Skin depth, δ (μm) at 2.45 GHz	Magnetic permeability, μ_r
Aluminium (Al)	3.69×10^7	1.7	1.00000065
Copper (Cu)	5.84×10^7	1.33	0.999994
Iron (Fe)	1.01×10^7	0.05	5000–6000
Gold (Au)	4.4×10^7	1.5	0.999998
Silver (Ag)	6.2×10^7	1.3	0.99999981
Tungsten (W)	1.79×10^7	2.4	1.000068
Cobalt (Co)	1.78×10^7	2.4	60
Lead (Pb)	4.8×10^6	4.7	0.999983
Magnesium (Mg)	2.3×10^7	2.2	1.00000693
Molybdenum (Mo)	2×10^7	2.4	1.005
Nickel (Ni)	1.4×10^7	2.7	50–600
Tin (Sn)	9.1×10^6	3.5	0.999993
Zinc (Zn)	1.7×10^7	2.5	1
Zirconium (Zr)	2.4×10^6	6.7	1
Titanium (Ti)	2.5×10^6	6.5	1.00005
Stainless-steel 316L	1.8×10^6	7.57	1.004
Stainless-steel 410L	1.75×10^6	0.2–0.3	700–1000

Surface roughness of the metal particle surface influences the overall electrical conductivity of metal particles, due to a rougher surface increasing the conductive channel of the surface current, increasing resistivity of the sample. As resistivity rises, the effective skin depth also increases as in Equation (4), increasing the sample's capability to absorb microwave energy. However, for particles with sizes $a \leq \delta$, yet still larger than the mean free path of electrons, ensures that the conductivity of a particle is equivalent to that of the bulk material. Non-spherical shapes such as cubes or stars should behave similarly to spherical particles. Hence, particle shape will have negligible effect on microwave heating, provided the particle size remains within the designated range [46,66]. Further study is required to gain a thorough understanding of the overall impact of particle shape on the microwave heating of metal particles. This is important as non-uniform metal particles (e.g. swarf, drill cuttings) will be a far cheaper metal processing feedstock than uniform particles.

2.6. Microwave hybrid heating – the role of susceptors

In material engineering, susceptor materials are classified as highly lossy (with tan $\delta > 0.01$) materials that function to absorb microwave energy and heat up quickly even at ambient temperature. In susceptor-assisted microwave heating, the processing material undergoes a dual heating process: first, the microwaves heat the susceptor, and then the heat is transferred to the sample surface via the conventional mode of heat transfer such as conduction. The susceptors raise the temperature of the load (or its container) to a required temperature level, causing the sample to become more absorbent and able to interact with the microwaves as the coupling temperature is attained. As the load temperature increases, it begins to interact with the microwave power and undergo greater and more uniform heating. This results in combination of conventional heating in the initial phase and microwave heating in later stages, thus it is termed hybrid heating. Table 1 gives a list of metals that have been processed using microwave power and indicates that most metals have a penetration depth of a few microns. Metal powder with a significantly larger size ($a \gg \delta$) is considered to be a coarser powder for microwave heating. When coarser metal powder particles are exposed to microwaves, only the surface layer of the particles absorbs energy and becomes heated within the particle's skin depth. The internal part of the

Table 2

Microwave energy absorption and penetration depth of selected materials at 2.45 GHz and room temperature unless stated [7,73–82].

Microwave susceptors			Microwave insulators/caskets		
Materials	Loss tangent, tan δ	Penetration depth, x (cm)	Materials	Loss tangent, tan δ	Penetration depth, x (m)
Silicon carbide (SiC)	0.37	1.93	Alumina (Al_2O_3)	0.001	12.65
			Al_2O_3 (1050 °C)	0.0138	
Graphite powder	0.36–0.67	1.34–2.09	Fused quartz	0.0003	75.73
Charcoal	0.14–0.38	6–11	Borosilicate glass	0.0012	15.7
Activated carbon	0.31–0.9	0.7–3.43	Teflon (PTFE)	0.00048	56.4
Carbon fibres	0.45–0.5	0.5–0.7	Mullite	0.0015	10.2
Carbon nanotube	1.11	0.2	Yttria stabilized zirconia (YSZ)	0.0011	>5
			YSZ (400 °C)	0.025	
Boron carbide (B_4C)[a]	0.01–0.08	×	PVC	0.0056	4.03
Boron nitride (BN)	0.085 (at 15 GHz)	×	Silicon (Si)	<0.012	>3.96
Titanium carbide (TiC)	>0.08	×	Silicon nitride (Si_3N_4)	<0.001	>12.2
Magnetite (Fe_3O_4)	>0.02	×	Boron nitride (BN)	<0.0005	>35
Boron carbide (B_4C)[b]	3.9	X	Zirconia (ZrO_2)	0.0043	>1
			Zirconia (1000 °C)	0.0531	
Boron Silicide (B_6Si)[b]	7.5	X	Aluminium Nitride (AlN)	0.005–0.008	×

*Unavailable or unclear values have been presented as " × ".

[a] The data source for this entry, (Fig. 3.17 [73]) does not show the temperature range or frequency (GHz) for the tan δ values reported.

[b] MW energy absorption per mole compared to water (1.0).

particle becomes heated by transfer of heat from the outer layer to the inner core of the particle through conduction. Microwave heating of coarser powders can encounter several issues, including reflection of the microwave power, arcing, thermal runaway, resulting in lack of reproducibility and uneven heating [49,67]. Susceptor-assisted microwave heating, often known as " microwave hybrid heating (MHH)" has been used in many studies to address these issues [7,68,69]. The successful design of MHH and effective use of microwave energy in metal processing is contingent upon three key factors: (1) the selection and design of a suitable susceptor material, (2) the selection and design of appropriate thermal insulation and load casket, and (3) proper positioning of the load within the microwave unit. Susceptor materials that are often used include carbon, charcoal, graphite and SiC [7]. The selection of a good susceptor material involves considering several factors to achieve efficient and effective heating. Key criteria for susceptor selection include a high dielectric loss factor tan δ for efficient conversion of microwave energy into heat, uniform heating to prevent hot spots and ensure even distribution, and thermal stability to withstand high temperatures.

Table 2 presents a list of materials and their loss tangents δ with potential for use as susceptors. Susceptors can be used in two ways: primarily as a crucible holding the load material or as secondary exterior block enclosing the load crucible. Microwave susceptible crucibles (MWSC) are generally more popular for metal melting applications and will be discussed in more detail in a later section. Secondary susceptors with different forms and shapes including powders, rods, tubes, and plates, have been reported [7].

Thermal insulation packages, often known as caskets, are additional crucial parts of MHH systems. The casket is designed to be transparent to microwaves and simultaneously act as both an insulator and containment that prevents heat dissipation from the load while withstanding high temperatures. It is more common to use ceramic materials with very low density and low loss factors for casket materials. The most frequently used insulating materials include porous alumina blanket, fibre wool, fire bricks, mullite, Teflon, quartz, silicon, yttria stabilized zirconia (YSZ) and boron nitride all of which have high microwave transparency (tan δ≪0.001) and thermal tolerances over a wide temperature range [7,83]. Table 2 lists materials that are microwave transparent and suitable for casket design along with their loss factors and penetration depths. Data at temperatures higher than room temperature indicate those materials, such as YSZ whose loss factors increase with temperature and transform to microwave susceptors.

Ceramic materials are essential components of many aspects of microwave metal processing serving as containment vessels, thermal insulation, transfer channels, ducts and susceptors in hybrid systems. The microwave susceptibility of a ceramic is defined as is tendency to heat internally when exposed to microwave radiation. Table 2 is a summary of the microwave susceptibility of selected ceramics as tanδ values. Values are at 2.45 GHz and room temperature unless stated. It is important to note that some microwave susceptible ceramics (MWSCs) do not absorb microwave energy at room temperature, however their microwave susceptibility changes as a function of temperature. In the case of some MWSCs, runaway thermal properties are encountered where susceptibility continues to increase as a function of increasing temperature. In the case of MWSCs that do not absorb at room temperature, admixture, or proximity to a MWSC that does absorb microwave energy at room temperature can be used to heat the second MWSC to a temperature where it does absorb microwave energy. For example, as discussed previously, SiC is such a primer MWSC or susceptor as it absorbs microwaves strongly at room temperature and above.

3. Applications of microwave in metals and metal alloy materials processing

3.1. Microwave sintering applications

The primary objective and scope of research on microwave power for metal processing was the sintering of metallic particles. The conventional sintering process comprises mixing material powder with additives or fillers, pressing into green parts, and then heating the green parts to allow diffusion in a conventional furnace such as a resistance furnace, induction furnace, or fossil fuelled furnace. Microwave sintering has been applied to sinter many commercial metal powders and alloys such as aluminium, copper, nickel, molybdenum, iron different grades of stainless steel and has been found to alleviate many of the drawbacks of conventional sintering methods. Microwave sintering has been proven as a superior method for metal processing offering efficiency gains and improved material performance across a diverse range of metals and alloys. It enhances heating rates, reduces processing times, and improves material properties. Microwave sintering has been shown to increase heating rates while decreasing processing times and saving energy [9]. This section will discuss the findings of microwave sintering of pure metal powder and selected alloys.

Microwave sintering of aluminium was compared to the properties of sintered parts produced through conventional heating [84] and demonstrated improved performance in microwave sintering over conventional sintering such as higher densification, lower porosity, and greater final tensile strength. Investigations into the sintering of pure
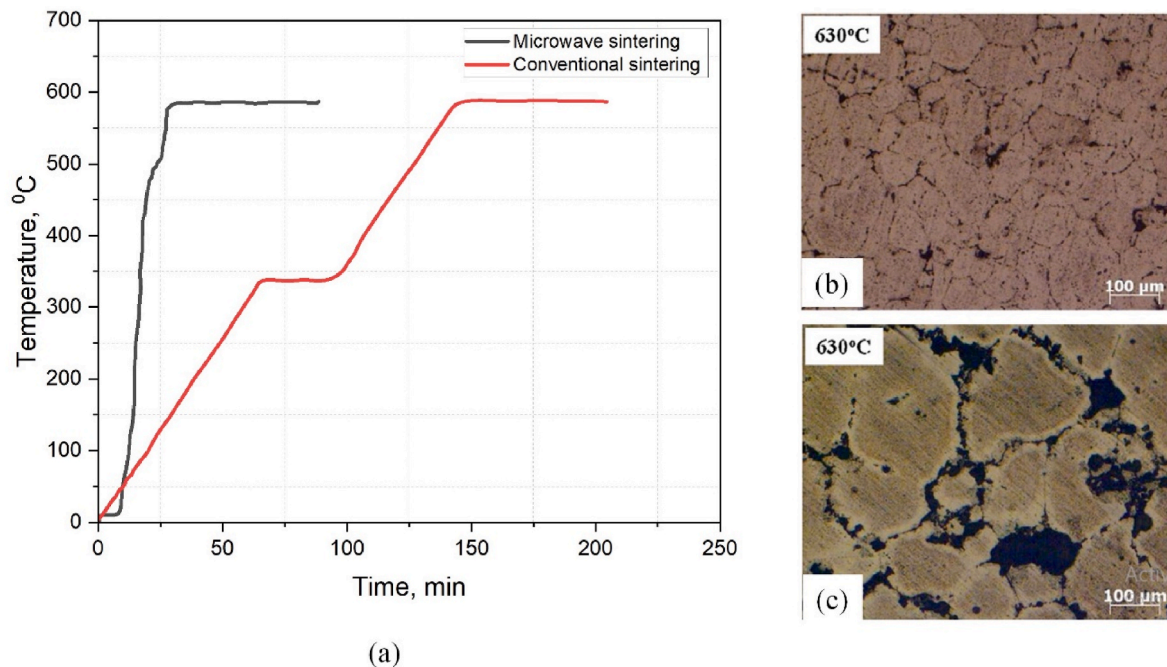
Fig. 5. (a) Comparison of the heating behaviour of aluminium alloy 6711 during conventional and microwave sintering; (b) optical micrographs images of 6711 sintered conventionally at 630^{0}C and (c) microwave furnace. Source: [93].

aluminium powder with an average particle size of 120 μm were conducted [85]. The microstructural evolution during microwave sintering was examined using synchrotron radiation X-ray computed tomography (CT) and results were compared to traditional sintering experiments. Distinct dominant diffusion mechanisms were observed, with microwave sintering showing grain-boundary and volume diffusion, while conventional sintering exhibited only surface diffusion. The effect of powder size on microwave sintering characteristics of pure aluminium powder [55] and concluded that larger (micron-sized) aluminium particles show a higher microwave heating capability than finer particles (nano particles) and the ratio of particle radius to skin depth is more important than particle size alone for conductive materials like aluminium. Numerous studies investigated the microwave sintering of aluminium alloys employing a hybrid microwave sintering setup using SiC powder as a susceptor [69,84,86–91]. Overall, results showed rapid sintering, a shortened processing time and reduced energy consumption that contributed to improved homogeneity in microstructure and hardness and compressive properties of aluminium metal matrix composites. However, some studies have shown that conventional heating methods outperform microwave heating in specific instances. For example, the impact of heating mode and sintering temperature on the sinterability and properties of the 6711 (Al–1Mg–0.8Si–0.25Cu) alloy was investigated [92]. Microwave sintering exhibited a significant (around 58 %) reduction in processing time compared to conventional methods, with higher heating rates in Fig. 5 (a). However, this rapid heating led to an inhomogeneous microstructure, characterized by larger melt fractions at grain boundaries, Whereas, conventional furnace sintering at 630 °C significantly improved microstructure Fig. 5 (b, c) and mechanical properties [93].

Based on the literature reviewed for this paper, copper and its composites are the most commonly investigated materials for microwave sintering. A 15 kW, 30 GHz microwave gyrotron system demonstrated enhanced densification of copper powder and alloys [94]. Densification initiated at the surface during particle neck growth due to elevated temperatures. Green density and extended soaking periods at the sintering temperature further enhance the final density. A similar 30 GHz gyrotron experimental set up was used by Mahmoud et al. [95], however they used three different sintering processing environments:

argon, nitrogen, and forming gas (mixture of 3H$_2$ + N$_2$). In addition to finding higher sintered densities with longer soaking times and higher green densities, they also discovered that best densification occurred with Ar gas. In a following work, Takayama et al. [96] demonstrated the feasibility of sintering copper compacts in air using microwave power without the need for an inert protective atmosphere. According to EDX results, microwave-sintered copper exhibits significantly less oxidation than conventionally sintered copper. Mondal et al. [27] used a 2.45 GHz multimode system to investigate the heating effect of copper powder particle size and sample initial porosity. Compacts with higher porosity and smaller particle sizes showed enhanced microwave coupling, faster heating, and higher densification in Fig. 6 (a, b). Demirskyi et al. [97–99] observed a distinct microwave sintering response in pure copper powder between single-mode and multimode applicators. While the multi-mode approach mirrored conventional sintering methods, the single-mode applicator exhibited superior performance. It facilitated faster and more uniform heating [Fig. 6 (c, d)], leading to considerably enhanced densification and even partial melting of the copper particles. The enhanced sintering of copper-based composites using the single mode microwave cavity has been investigated in several studies [28,44, 100].

Sample pellets of various sizes and shapes were produced by cold pressing pure iron powder with a small amount of binder on the sintering of iron powder and its alloy composites [94,92,101,102]. A specially designed multimode microwave furnace operating at 2.45 GHz with an output power of 6 kW was used, allowing temperature to be varied from ambient to 2273 K. Yttria- and zirconia-based insulation was used to preserve the heat within the furnace and SiC and MoSi$_2$ susceptors were used during the sintering process [11]. In comparison to the conventionally sintered samples, microwave-sintered parts showed finer microstructure, higher densification, hardness and increased transverse rupture strength (TRS), and modulus of rupture (MR) [94, 92]. Nadjafi et al. [103] conducted sintering of Fe and Fe–Cu powder compact samples using both microwave and electrical tube furnaces. Microwave-sintered materials have shown finer microstructure, 6–8 % higher density, a 5–10 HV$_5$ hardness increase, and a 10 % increase in tensile strength in comparison to the electric furnace. Anklekar et al. [104] observed better mechanical characteristics and microstructural
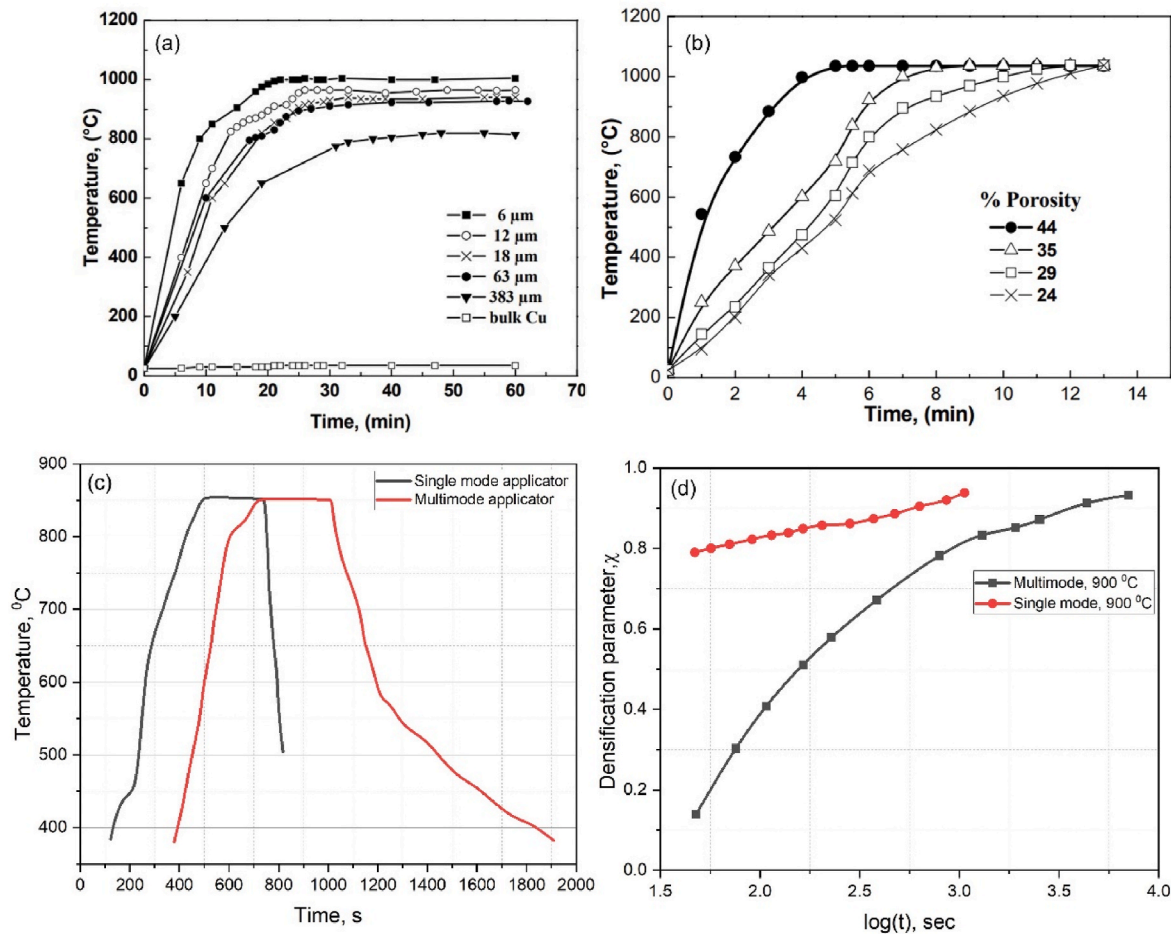
Fig. 6. (a) Effect of different particle sizes on the heating performance of Cu compacts in a microwave furnace, (b) Effect of changing the initial porosity on the heating behaviour of Cu compact. Source: [27], (c) Temperature profiles of microwave sintering of copper using multimode and single mode applicator; (c) Densification kinetics of copper samples heated by single-mode and multi-mode microwaves cavity. Source: [98].

development with hybrid microwave sintering of the steel-copper alloy (97 % Fe, 2 % Cu). Several other works [44,105,106] reported microwave sintering of iron powder with decreased process time and increased densification.

The effects of microwave and conventional sintering on ferritic (434L) and austenitic (316L) stainless steel was investigated and achieved [107]. When compared to conventional sintering a 90 % reduction in processing time was achieved at a slow heating rate (278 K/min) and isothermal holds at intermittent temperatures in a conventional furnace. The enhanced microwave sintering of different grades of stainless-steel powder has been reported by several other studies [108–115].

Demirskyi et al. [116] investigated sintering of pure Ni powder using a 6 KW multimode cavity operating at 2.45 GHz without susceptors. The results revealed an anomalous rate of sinter neck growth and the production of a liquid phase during microwave sintering. Several studies have reported microwave sintering of nickel composites such as nickel steel [104], versatile Ni–Zn ferrites [117–120], W–Ni–Fe alloys [121, 122], and other nickel alloys [68,123–125].

Prabhu et al. [126] demonstrated the feasibility of microwave sintering of pure tungsten powder with average particle size of 5–7 μm using a 3 kW multimode microwave furnace with a process duration of 6–7 h and a maximum power consumption of 20 kW. With 85 % green density, the sintered compact achieved 93 % of the theoretical density. Wang et al. [127] achieved microwave sintering of tungsten at a comparatively low temperature of (1673–1773 K) in a relatively short period (30 min) while also achieving a relatively higher density of 93.5 % with ball milled micrometre (3 μm) and nanoscale (20–100 nm)

powders. They introduced some impurities into the W powder, such as Fe and Cr, during the ball milling process. Improved microstructural and mechanical characteristics of microwave-sintered WC/Co composites were reported by several research [35,128].

Several efforts have been undertaken to investigate the effect of reinforcements on the mechanical and microstructural behaviour of magnesium [129–131]. The pioneering work in this field [132–134] research on the hybrid microwave sintering of pure magnesium powders and investigated the effect of reinforcements on the mechanical and microstructural behaviour of magnesium. It was shown that the hybrid microwave sintering using SiC susceptors significantly reduced the sintering time by up to 85 %, and improved hardness and tensile properties over conventionally sintered magnesium. Sethi et al. [135] investigated the process of sintering bronze Cu–12Sn in a protected environment using microwave and convection heating. Results revealed that microwave sintering of bronze powder reduced processing time by more than 50 %. Another significant difference is that premixed bronze compacts "swell" at high temperatures (1048 K) during conventional sintering, but no swelling occurs during microwave sintering of premixed and pre-alloyed compacts. Swelling is a common phenomenon in traditional powder metallurgy processes that opposes sintering, resulting in de-densification and irregular porosity evolution [136]. Swelling in ceramic systems such as Al_2O_3 or ZnO is caused by the escape of gas trapped in the green compact when the inner pressure exceeds the sintering force [137].

Sato [138] experimentally investigated the heating processes of titanium and titanium oxide powder during microwave heating from the
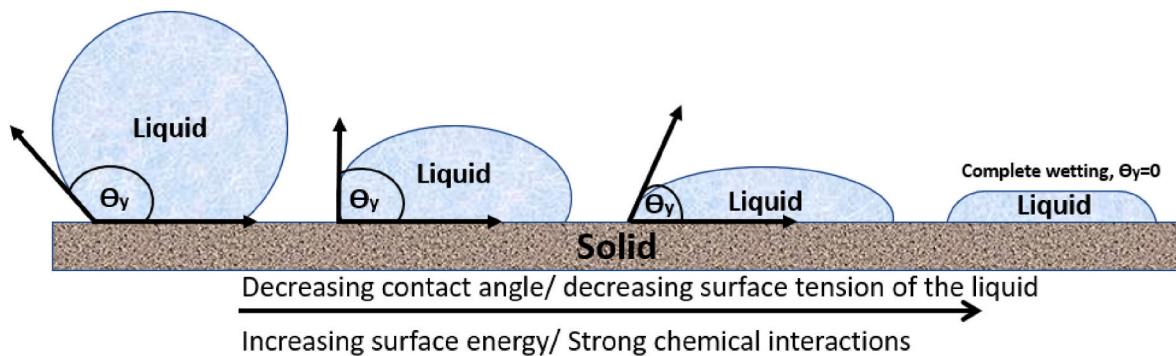
Fig. 7. Definition of contact angle in respect of a liquid metal and solid ceramic. Source: adapted from Ref. [160].

perspective of the interaction between the magnetization of the material and the microwaves. They found that loose Ti (99.5 % pure, 50 μm) powder responded weakly to pure microwave radiation when exposed to a single mode applicator with 300 W output. The temperature of pure Ti did not rise above 473 K after 2 min of exposure to either the E or H field, but TiO was quickly heated to 1223 K in the E-field within 10 s. The poor response of Ti powder to microwaves was attributed to its paramagnetism. A similar observation was made when Ti powder was heated in a multimode 2.45 GHz microwave applicator at 1000 W for 60 s [139], as the temperature scarcely increased from 293 K to 313 K. Luo et al. [140,141] attempted microwave sintering of pure Ti particles using susceptors. The hybrid microwave heating with the surrounding SiC or MoSi$_2$ susceptor increased the heating of Ti powders to 1473 K in less than 90 min at 0.3–0.8 kW input power and achieved sintered density of 96.3 % of theoretical density. Several publications reported that the use of a susceptor can significantly enhance the heating and sintering effectiveness of Ti-based powders, as well as provide a steady and controlled heating process [142–145]. Nivedhita et al. [146] demonstrated that adding Ni (150 μm, 99 % purity) to TiC(325 μm, 99 % purity) increased density at comparatively low temperatures (1200 °C). Recently, there has been a growing interest in using nonconventional synthesis methods, particularly microwave heating, in the development of thermoelectric and magnetic materials for energy-related applications [3,147–149]. Thermoelectric materials can transform waste heat into useable electricity, contributing to energy savings and efficiency. Producing thermoelectric metals like TiNiSn and TiCoSb poses challenges because of their different melting points lead to with microstructure and phase purity in conventional preparation methods. Microwave heating has been demonstrated as a successful rapid and energy-efficient approach that overcomes incompatibilities related to microstructure and phase purity [150].

3.2. Microwave melting and casting applications

The use of microwave-assisted heating systems has demonstrated potential in the processes of melting and casting metals and metal alloy materials [21,151]. Metals such as uranium, titanium, aluminium, steels, copper, bronze and other metals and alloys with varying volumes and masses ranging from a few kilogrammes to 350 kg have been melted using susceptors [152,153]. Chandrasekaran et al. [154] reported melting of a small quantity of various metal powders (including tin, lead, aluminium and copper) in a graphite crucible using a 1.3 kW multimode microwave furnace and a SiC susceptor. In comparison to conventional furnaces, microwave melting was found to be twice as fast, use less energy, and was safer to operate. Mishra et al. [155,156] developed a method of in situ casting of metal using an industrial multimode microwave oven with a power of 1.4 kW and a frequency of 2.45 GHz. The setup was constructed using materials that interact well with microwaves, including a pouring basin with a SiC susceptor, an alumina sprue, and a two-piece graphite mould. The setup melted a

100g cylindrical piece of aluminium 7079 alloy in only 8 min and 45 s. Xu et al. [157] melted copper powder of various sizes using microwave power in the absence of susceptor materials. Several studies investigated the feasibility of microwave melting of bulk metallic materials, and it has been suggested that this method is more efficient than other conventional methods [156,158]. Sun et al. [159] experimented the effect of microwaves on liquid and found that microwave irradiation did not heat molten metals.

3.3. Non-wetting of microwave susceptible ceramics in microwave metal processing

For melting and casting metals using microwave susceptible ceramic (MWSC) containments should possess a non-wetting (NW) quality, which indicates that the MWSC does not react with the molten metal. It is essential that the MWSC has this characteristic to successfully cast the metal object without alteration, deterioration, or contamination of the metal being processed. Conversely, it is undesirable if for MWSC's to be weakened over time due to its interaction with the metal. The intrinsic ability of a non-reactive liquid to wet a smooth chemically homogeneous surface is quantified by the value of Young's contact angle Θ_y, which is a characteristic of a solid-liquid-vapour system. Fig. 7 shows the relationship between contact angle Θ_y and liquid wettability.

The contact angle (θ_Y) between a liquid metal and a solid surface is a measure of the wetting behaviour of the liquid metal on the surface. When the contact angle is greater than 90°, it indicates that the liquid metal does not wet the surface well and has weak physical bonding with it. In contrast, a contact angle less than 90° indicates that the liquid metal wets the surface well and has strong chemical bonding with it [161]. In microwave metal casting, a high contact angle ($\theta_Y \gg 90°$) or non-wettability is necessary to indicate that the metal does not react with the mould surface. Tables 3 and 4 shows the wettability of molten metal-MWSCs for various ceramic materials. Tables include information on the Young's contact angle (if available) and the temperature at which the observation was made. However, some references only provide a qualitative indication of wettability or non-wettability.

Fig. 8 is a plot of microwave energy susceptibility plotted against metal wettability of the given metal with the given MWSC taken from Tables 3 and 4 The plot does not identify the microwave frequency or energy output and therefore serves a general guide and indication of the overall behaviour and selection of Metal-MWSC pairs that may be useful in metal processing. Note that some MWSCs do not absorb microwave power at low temperatures but become so at higher temperatures. Fig. 8 shows up to 40 possible matching candidates, however, the results shown are not exhaustive.

3.4. Microwave cladding and coating applications

Cladding is a process in which a layer of metal powder is deposited onto the surface of a substrate material by partially melting the substrate

Table 3
MWSC ceramic materials and their wettability by various molten metals.

Microwave Susceptible Ceramic (MWSCs) Materials

Metal	Silicon Carbide (SiC)			Zirconia (ZrO$_2$)			Yttria Stabilized Zirconia (YSZ)			Alumina (Al$_2$O$_3$)			Aluminium Nitride (AlN)		
	Wettability	Contact angle (deg)	Ref	Wettability	Contact angle (deg)	Ref	Wettability	Contact angle (deg)	Ref	Wettability	Contact angle (deg)	Ref	Wettability	Contact angle (deg)	Ref
Ni	Yes	12.2 at 1013 K	[161]	Non	90 at 1744 K	[162]	Non	122.33 at 1740K	[163]	yes	11.6 at 1013 K	[164]	Non	>90 at 1744 K	[165]
Sn	Non	165 at 1473K	[166]	Non	>100 at 1546 K	[167]	Non	>140 at 973 K	[168]	yes	60 at 1213 K	[169]	Non	×	[170]
Al	Non	134 at 1073 K	[171, 172]	Non / Yes	110 at 973 K / 55 at 1373 K	[161]	Non	145 at 1173K	[167]	Non	126 at 953K	[173]	Non	102	[173]
Ga	×	×	×	Non	160	[162]	×	×	×	×	×	×	×	×	×
In	Non	130	[174]	Non	125	[162]	×	×	×	Non	124	[174]	×	×	×
Ag	Non	140 at 1223K	[175]	Non	126	[162]	Non	135 at 1273K	[167]	Non	144	[174]	Non	×	[176]
Au	Non	150–110 at (1336–1703) K	[166]	Non	125 at 1423 K	[162]	Non	>90	[177]	Non	138	[174]	Non	130	[176]
Si	Yes	54–30 at (1673–1773) K	[166]	Non	125 at 703 K	[162]	×	×	×	Yes	86 at 1693K	[178]	Yes	40 at 1683 K	[179]
Ge	Yes	42 at 1473 K	[166]	Non	95 at 1273 K	[162]	×	×	×	×	×	×	×	×	×
Co	Yes	63 at 1803K	[166]	Non	105 at 1773 K	[162]	×	×	×	Non	114	[174]	×	×	×
Fe	Yes	50 at 1633K	[175]	Non	93 at 1823 K	[162]	×	×	×	Non	141	[174]	×	×	×
Ti	Yes	<40 at 1773 K	[166]	Non	103	[180]	Non	170 at 1973K	[181]	Yes	<90	[182]	Yes	80	[179]
V				Yes	65	[162]									
Cu	Non	165 at 1723 K	[166]	Non	130 at 1373 K	[162]	non	122 at 1473K	[163]	Non	120 at 1523K	[175]	Non	×	[179]
Pd	×	×	×	Non	98 at 1833 K	[182]	×	×	×	×	×	×	×	×	×
Pt	×	×	×	Non	93 at 2073 K	[182]	×	×	×	×	×	×	×	×	×
Rh	×	×	×	Non	105 at 473 K	[182]	×	×	×	×	×	×	×	×	×

Notes to Table 3.
*Unavailable or unclear values have been presented as " × ".
"Non" means non or low wettability or implies reactivity.

Table 4
Metal-MWSCs wettabilities for BN, TiC, and TiB$_2$.

Metals	Microwave Susceptible Ceramic (MWSCs) Materials		
	BN	TiC	TiB$_2$[a]
Al	Non (133° at 1373K) [183]	Non (118° at 973 K°C) [184]	Non (95° at 973 K) [185]
Ag	X	Non 125° at 1263 K [176]	X
Ag–Ti Alloy	Hi Reactivity of the Ti [186]	X	X
Cu	X	Non 130° at 1373 K [176]	X

Notes to Table 4.
*Unavailable or unclear values have been presented as " × ".
"Non" means non wettability or low wettability, (or reactivity).
Contact angle θ$_Y$ shown if known and reported.
[a] Titanium Diboride (TiB$_2$) is an electrically conducting ceramic and can be machined using electron discharge machining (EDM).

and entirely melting the selectively added powder on the substrate. In metallurgy, cladding is used to create coatings with minimal dilution of the substrate or base material that improve the durability and performance of parts and components, as well as to repair damaged or worn surfaces [187]. Metal cladding has a wide range of applications, including aerospace, automotive, oil and gas engineering, electronics industries, and agricultural applications [188,189]. There are numerous surface engineering techniques for creating surfaces with specific properties, notably thermal spraying, tungsten inert gas (TIG) cladding, and laser cladding, which can be used for both practical and competitive

purposes. Laser cladding is the most adopted method, in which a laser beam is used to melt a coating material onto a substrate. The coating material is normally in the form of a powder or wire, and the laser beam melts the material onto the surface of the substrate, forming a metallurgical bond. Despite its advantages, laser cladding has some drawbacks such as its high installation and operating costs, as well as the development of thermal residual stresses caused by localized thermal distortion [190].

Gupta et al. [187,191–196] developed microwave cladding process and the characterisation of the resulting composites using microwave hybrid heating to produce Cu and Ni-based powder (EWAC) coatings on austenitic stainless-steel substrate. Microwave cladding process was carried out using a domestic multimode microwave with a power output of 900 W at a frequency of 2.45 GHz for 360 s. The EWAC powder was first dried out by heating it in a conventional furnace for 24 h. The powder was then manually applied to a stainless steel-316 substrate with a relatively consistent thickness (1 mm). To heat the powder, the hybrid heating technique was used, which involved placing a susceptor (charcoal powder) on top of the cladding powder separated by a graphite sheet. Fig. 9 illustrates the concept of cladding process using microwave power. The microstructure and mechanical characteristics of developed clads were analysed through several techniques, including field emission scanning electron microscope (FE-SEM), energy dispersive X-ray spectroscope (EDS), X-ray diffraction (XRD) and Vicker's micro-hardness measurement [190]. The microstructure properties of microwave cladded metal parts can vary depending on the cladding materials used and the cladding process parameters. The results showed that, despite the presence of limited micro pores (<1 %), the microwave cladding produced a fine-grained structure and desirable properties such
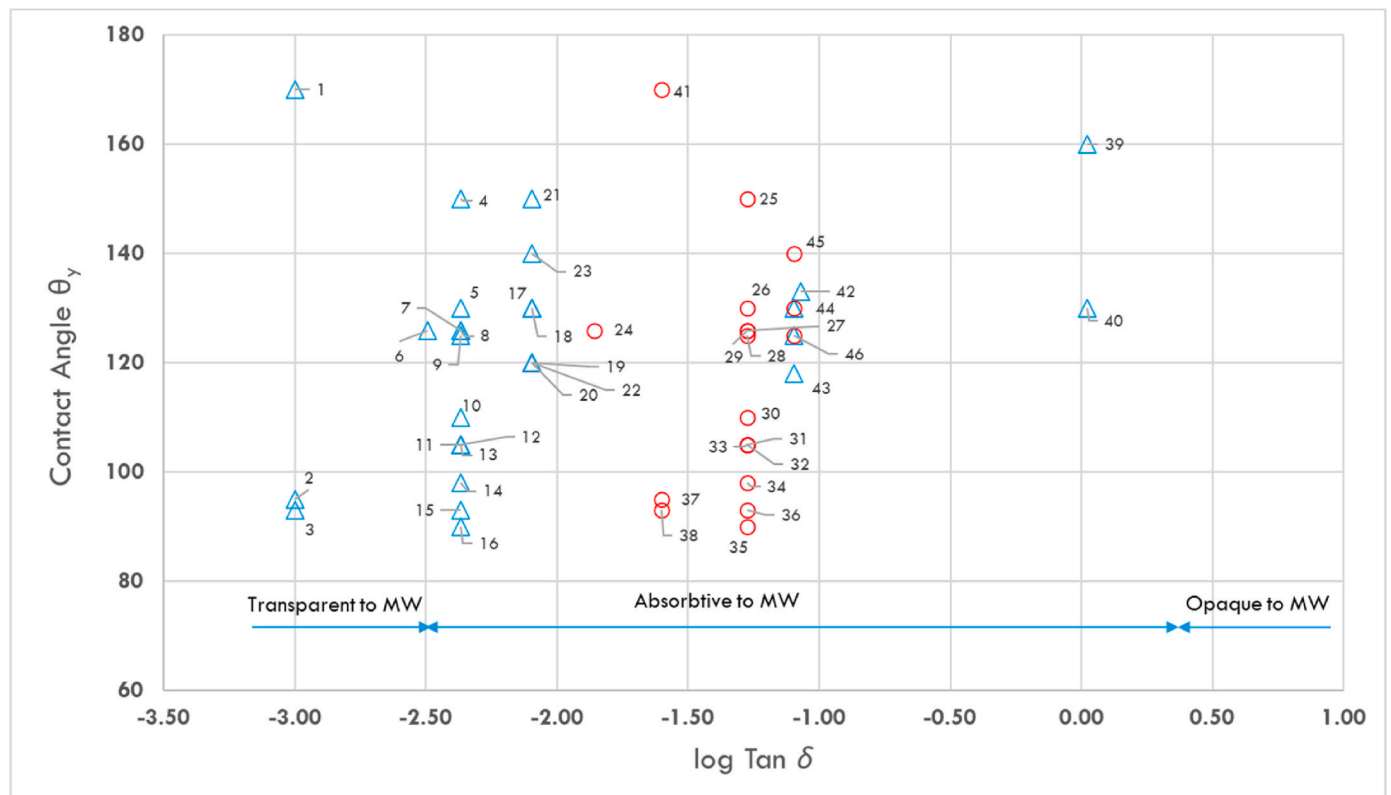
Fig. 8. Compilation of data on microwave energy susceptibility (as log Tan δ) against metal wettability as Contact Angle Θ$_Y$ for the given MWSC-Metal pair at nominally low temperatures (open triangles) and high temperatures (open circles). Tan δ data plotted as logarithm purely for data presentation. References in Table 3. Key to the Metal-NW-MWSC pairs [1]: Ti – YSZ (8mol %) [2]; Ge – YSZ (8mol %) [3]; Fe – YSZ (8mol %) [4]; Ga – Zirconia [5,6]; Al – Alumina [7]; In – Zirconia [8]; Ag Zirconia [9]; Au – Zirconia [10]; Al – Zirconia [11]; Co – Zirconia [12]; Si – Zirconia [13]; Rh – Zirconia [14]; Fe - YSZ [15]; Pt-Zirconia [16,17]; Cu – SiC [18]; Al–AlN [19]; Sn (solder) - AlN [20]; Cu–AlN [21]; Ag - AlN [22]; Ge-AlN [23]; Ni–AlN [24]; Al - Alumina [25]; Ga - Zirconia [26]; Cu - Zirconia [27]; In - Zirconia [28]; Al - Zirconia [29,30]; Al - Zirconia [31]; Si - Zirconia [32]; Co - Zirconia [33]; Rh -Zirconia [34,35]; Fe - YSZ [36]; Pt - Zirconia [37]; Ge - YSZ [38]; Pt - Zirconia [39]; Al–SiC [40]; Cu–SiC [41]; Ti – YSZ. Source: Authors.
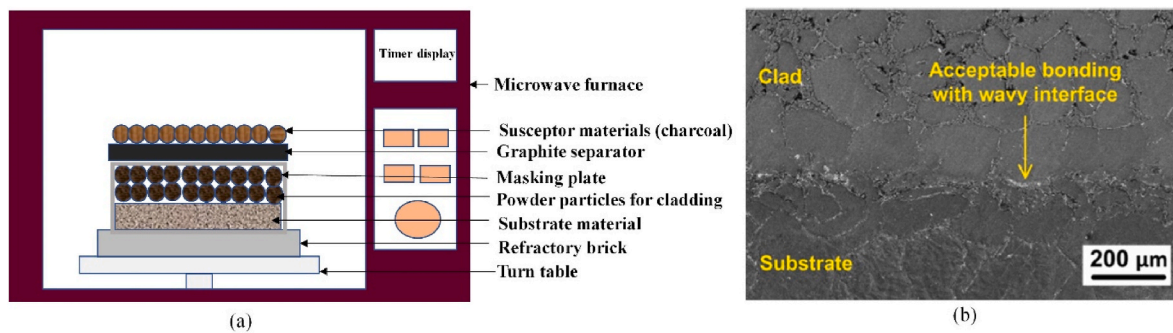
(a)

(b)

Fig. 9. (a) Schematic of microwave hybrid heating approach for cladding process, (b) SEM micrograph illustrating clad-substrate interface. Source: [197].
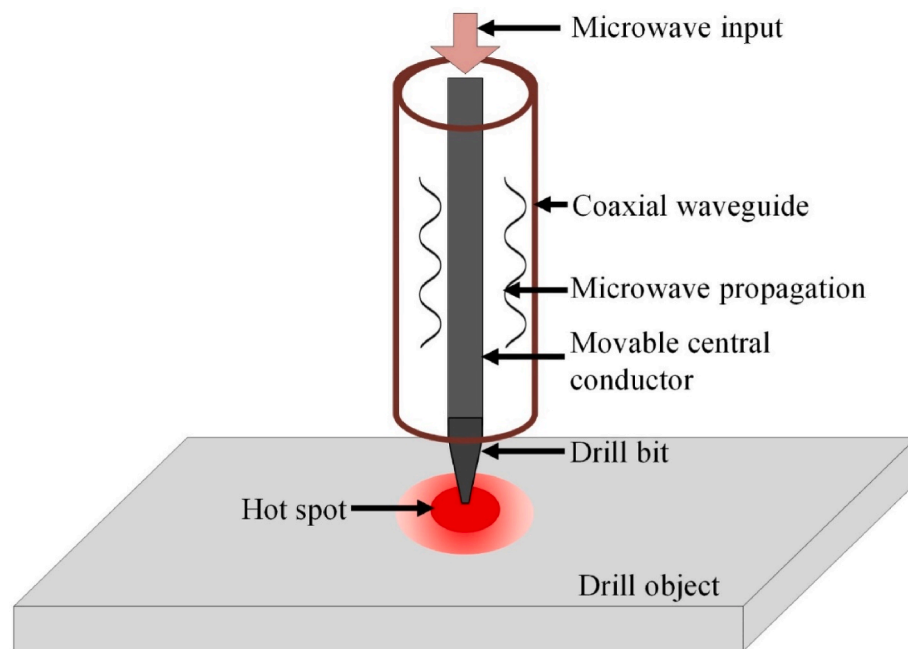

Fig. 10. (a) Schematic illustrating the principle underlying the operation of a microwave drill. Source: adapted from Ref. [207].

as uniformity, density, and high micro-hardness on the stainless-steel substrate.

Zafar et al. [198–201] demonstrated improved micro-hardness properties of the stainless steel 304 substrate through microwave cladding of Inconel-718 (nickel-chromium alloy) and WC-12Co (cermet based) clads using a domestic microwave applicator at 2.45 GHz and 900 W. The microstructural analysis of the Inconel-718 clad revealed a good metallurgical bond with the partially molten substrate surface and no apparent interfacial cracking.

Microwave hybrid heating method was used to explore the size effect of WC-12Co micrometric (MM) and nanometric (NM) clads on SS304 substrate [201]. The NM WC-12Co microwave clad outperformed its micrometric counterpart in terms of wear resistance (54 % reduction in average weight loss). The improved sliding wear resistance of the NM microwave clads was attributed to the homogeneous distribution of the nano carbides and enhanced microhardness of the clad layer [202]. The enhanced microwave cladding of various configurations of Ni, WC, SiC, and Mo-based clads on various grades of stainless-steel substrate has also been investigated in several works [202–205].

3.5. Microwave drilling applications

Drilling is a critical operation in many industries, such as manufacturing, construction, mining, and oil and gas, as it enables the creation of holes in different materials, including metal, wood, plastic, and concrete, to various sizes and depths. Research shows that drilling procedures can consume a significant portion (25 %) of manufacturing time, thus manufacturers are constantly seeking ways to improve drilling efficiency and accuracy [206]. Among the relatively new non-conventional techniques, various laser-based drilling methods have been claimed to be widely used in industry. While other non-conventional drilling methods such as Electro discharge machining (EDM), Spark assisted chemical engraving (SACE), Electron beam (EB), and ultrasonic vibration have also gained attention among researchers, laser-based drilling is particularly notable for its capacity to achieve high precision and high aspect ratio micro drilling applications. However, laser-based drilling typically requires expensive solid-state laser sources, which can contribute to significant operation and maintenance costs [206]. Jerby et al. developed a non-conventional microwave drill that merged the precision and cleanliness of a laser drill with the affordability of a mechanical drill [207]. The microwave drilling method is based on the concept of Localised Microwave Heating (LMH), which concentrates microwave energy into a small hot spot, resulting in the formation of a thermal runaway within the material to be drilled [208]. The microwave drill schematic shown in Fig. 10 is essentially an open-end coaxial waveguide with a moveable centre electrode (tungsten rod) fed by an adjustable 1000 W, 2.45 GHz magnetron [207]. Open-ended coaxial applicators concentrate microwaves locally, and
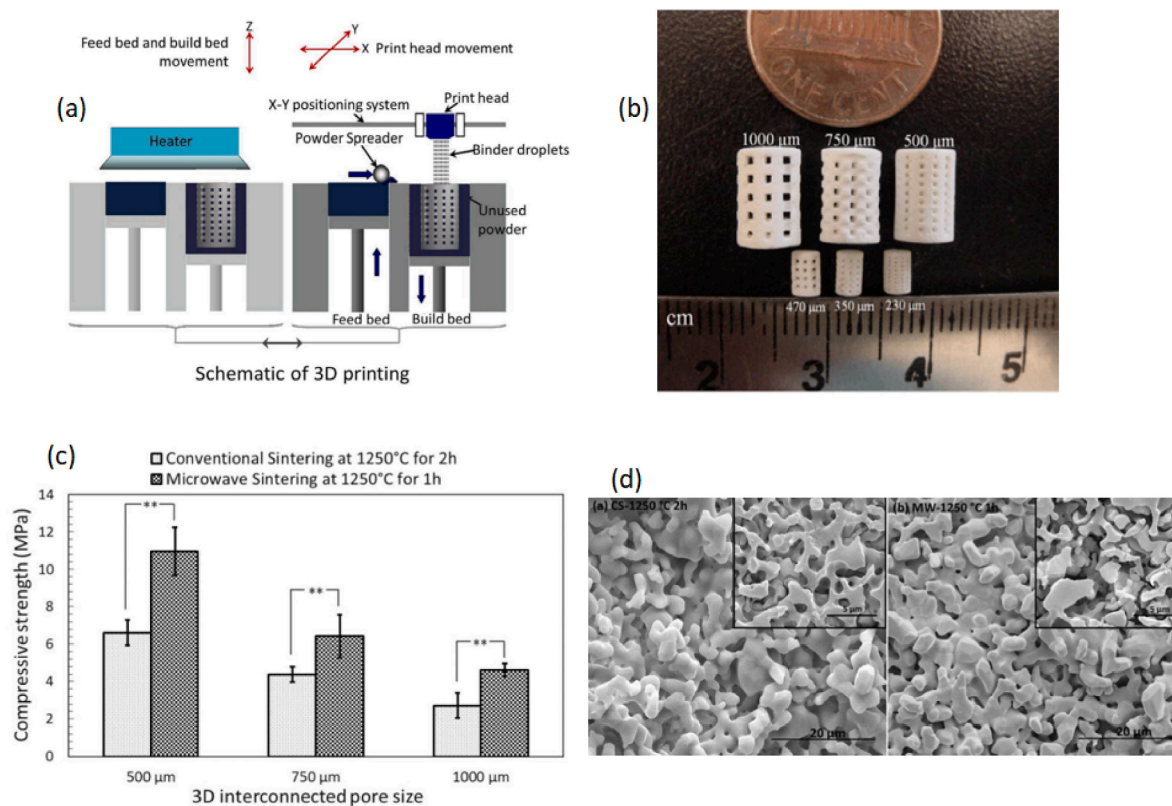
Fig. 11. (a) Schematic of 3D printing process, (b) Photo of sintered 3D printed scaffolds with varied microchannel, (c) Strength comparison of scaffolds sintered at 1250 °C in conventional and microwave furnaces, (d) SEM images depict the surface morphology of sintered scaffolds. Source: [238].

because materials that are hotter tended to absorb microwaves more efficiently, this resulted in greater energy absorption in the subsurface. Consequently, the material softened or melted, and then the central electrode was inserted into the softened area to shape the hole's boundary. Microwave drilling has been demonstrated for a variety of materials, including ceramics, glass, bone, concrete, basalt, silicon, and polymer [209–211]. For example 2-mm-diameter holes 2 cm deep were drilled in concrete in less than a minute each, able to create 1 mm diameter holes in ceramic and glass plates [212]. Jerby et al. [213] also demonstrated a solid-state microwave drill that operates at relatively low microwave power in the range 10–100 W. Small shallow holes were created (a few mm in diameter and depth) in various materials such as glass, ceramics, and basalt. George et al. [214] first reported microwave drilling of metal sheets. To create a hole, they employed a charcoal susceptor-based microwave hybrid heating approach. They concentrated the microwaves at the tip of a metallic drill bit that was in contact with the workpiece via the charcoal susceptor. This caused the targeted area to soften. Then, a tungsten drill bit that was spring-loaded applied pressure to the softened area to create the hole's boundaries. Al, Cu, and stainless-steel sheets were drilled to 1 mm thickness using a 2 mm diameter tungsten drill bit for 120, 150, and 240 s, respectively at 2.45 GHz and 900 W. The performance of different drill bit and importance of selecting drill bit materials that can efficiently absorb and utilize microwave energy for specific drilling applications were investigated [215]. Seven types of different drill bits were used, made of steel and copper for drilling holes in perspex (PMMA). The results showed that copper drill bits were more effective, with better hole quality and less tool wear compared to steel drill bits. Singh et al. attempted microwave drilling on galvanized steel and stainless steel sheets with thoriated tungsten as drilling tool in a domestic microwave at 700 W, 2.45 GHz [216]. The results revealed issues such as undercut, irregular, and overcut hole profiles in both sheets, attributed to non-uniform heat dissipation and tool wear. discussed microwave metal discharge-based

microwave drilling of galvanized steel and stainless-steel sheets inside a domestic microwave applicator with a rated power of 700 W and a frequency of 2.45 GHz. Further study is needed for gaining a deeper understanding and enhancing precision in microwave drilling processes to achieve improved accuracy and repeatability.

3.6. Microwave joining applications

Microwave joining of metal, also known as microwave welding, is an alternative to traditional welding methods such as arc welding or resistance welding. A wide range of materials, including polymers, ceramics, different grades of steel, copper in various shapes and forms, and interface material in the form of powder slurry, have been investigated for their potential in joining using microwave energy [21,217–221]. Microwave joining of dissimilar metals is difficult to achieve using conventional welding methods [222]. Srinath et al. [223] reported microwave joining of bulk copper plate by using copper powder (5 μm) mixed with epoxy resin (slurry) as the joining medium. Subsequently, they used the same microwave hybrid heating setup with a charcoal susceptor to successfully join stainless steel-316 plates with a nickel-based powder slurry in 390 s [224]. Inconel-625 alloy was joined in 21 min and join Inconel-625 plates with Inconel-625 powder slurry in 21 min [225,226]. Many successful joints have been made between metals and alloy through microwave hybrid techniques using variety of susceptor and filler materials [225,227–232].

3.7. Microwave additive manufacturing and 3D printing applications

Microwave power has potential in additive manufacturing (AM) and 3D printing of metals and their alloys. Traditionally in metal additive manufacturing, a high-powered laser or an electron beam is employed as the heat source, fusing and sintering the metal powder layer by layer to make a solid 3D object [233]. E. Jerby et al. [234] first demonstrated the

feasibility of incremental solidification of metal powders for AM of 3D structures using a localized microwave heating technique. The process involved depositing bronze-based metal powder with a fine grain size onto a substrate, similar to the approach used in laser-based rapid prototyping systems. However, instead of a laser, a coaxial applicator powered by magnetron-based generator at 2.45 GHz at 1 kW was used to heat and melt the powder.

Shelef and E. Jerby et al. [235] also reported a method for microwave heating of small batches of ferromagnetic metal powders in a contactless magnetic confinement for AM purposes. An external magnetic field (3 mT) was used to retain the iron-based compacted powders in the form of a voxel within the microwave chamber. Each voxel was transformed into a molten state through plasma discharge caused by 2.45 GHz, 1 kW microwave radiation, subsequently solidified into a bead and gradually merged with the previously formed structure.

Subsequently, Shelev and Jerby [236] demonstrated the feasibility of using a solid state microwave system for melting and incremental solidification of metal powder for additive manufacturing. This method was subsequently demonstrated for sequentially melting and solidifying metal powder using a lateral scanning approach [237]. Overall, the microstructure and mechanical characteristics of this processing method showed comparable density and hardness compared to laser-based AM techniques.

Some 3D printing processes use binders to form the green parts of 3D printed objects. Microwave heating has been found to be a faster and more efficient method of removing the binder than traditional binder removal methods, such as thermal debinding or solvent extraction [238, 239]. M Salehi et al. [240] demonstrated the use of microwave sintering to densify centimetre-scale Mg-based alloys for binder less 3D printing applications. Findings showed that the duration of the binder removal and sintering was shortened three-fold compared to conventional sintering [240,241]. Tarafder et al. [242,243] reported microwave sintering increased the mechanical strength of 3D printed porous tricalcium phosphate scaffolds shown in Fig. 11 (b). The 3D printed scaffolds with 500 μm green porosity were sintered at 1250^0C in microwave and conventional furnaces. Microwave sintering achieved a considerable improvement in porosity of 400 μm pores in the scaffolds after sintering as well as increase in compressive strength 11 ± 1.3 MPa, which is between 46 % and 69 % higher than conventional sintering shown in Fig. 11 (c) [242]. Li et al. [244–246] developed 3D printing technique in which microwaves were utilised to heat metal-like continuous carbon fibre. They designed a coaxial resonant microwave applicator that melted carbon fibre while simultaneously increasing its mechanical strength.

4. Current challenges, issues, and future scope in microwave metal processing

Incorporating alternative technologies into industrial processes is vital for addressing environmental challenges and facilitating the transition towards a more sustainable future. The use of microwave heating as an alternative to conventional heating in metallic material processing has benefits such as ease of processing, reduction of processing time and energy savings, and improved quality of the processed parts. Although there are several essential benefits associated with utilizing microwave heating in the processing of metallic materials, there are also certain challenges and issues that must be studied and resolved to extend its use to a wider array of applications. The primary challenges related to microwave processing of metallic materials are establishing the geometry of the power supply and tuning system, establishing a stable microwave power supply, preventing microwave reflection and impedance matching, temperature control, plasma formation and thermal runaway, material handling with varying electromagnetic properties, equipment design and scaling up of microwave-based processes.

4.1. Establishing stable microwave power supply

Despite the numerous publications and arguments supporting the positive effects of microwave technology, the industrial and manufacturing sectors remain hesitant to adopt it as an alternative technology. The reluctance stems from the need for convincing evidence of efficient and stable energy transfer ensuring the highest levels of performance, reproducibility, and reliability in the final product. Achieving an efficient microwave transfer system necessitates a comprehensive understanding of microwave physics, power supply design and architecture, tuning, collimation, system geometry, as well as the precise delivery and control of power. The operation and challenges associated with microwave equipment commence with the generation of microwave power. There are two distinct technologies for microwave generation: magnetron and solid-state generators, each presenting unique difficulties. The generation of microwave radiation relies on a high-voltage power supply and a power converter necessary to elevate the mains supply voltage to levels required by the magnetron. Achieving precision and stability in the power converter is challenging due to inherent frequency harmonics, external factors such as temperature variations, and power supply fluctuations contributing to frequency instability. Attaining precise control over the output power and frequency of a magnetron also poses challenges. Magnetrons can generate significant heat during operation leading to energy loss. Efficient cooling is essential to prevent overheating and ensure optimal performance, introducing complexity and increasing the overall cost of system. A 2.45 GHz magnetron of high quality can have an electrical efficiency of approximately 70 % and at 915 MHz can achieve around 90 % [247]. Practically, generating a 5-kW microwave output power at 2.45 GHz would necessitate ~7.04 kW of grid electrical power. Alternatively, solid-state microwave generators that rely on semiconductor-based power amplifier technology offer notable advantages over conventional magnetron-based systems, including precise control over frequency, phase shift capabilities, and enhanced power combining. While solid-state technology presents new opportunities, it also poses challenges such as maintaining consistent frequency and controlling relative phase among sources. The complexity of RF circuits and materials contributes to a higher cost two to four times per watt compared to magnetron-based units, and achieving higher output microwave power remains a challenge; currently, the maximum output of a single unit is 1 kW at 2.45 GHz with power efficiencies ranging from 30 % to 60 %.

4.2. Microwave transmission and impedance mismatch

Ensuring efficient microwave power transfer to the sample load is crucial for process energy efficiency and safety. Challenges in microwave transmission involve maintaining efficient and loss-free power transfer, addressing material considerations in commonly used waveguides and coaxial cables (primary MW transmission lines) to handle power losses, and addressing safety concerns associated with reflected power. According to transmission line theory, the maximum power dissipated in the load material occurs when the impedance of the load material being processed and that of the cavity wall equals the impedance of the source (generator), otherwise there will be reflected power, P_r. Measurement and control of P_r are critical for the safe and efficient operation of microwaves, where the difference between forward power (P_f) and reflected power (P_r) offers an estimate of the power absorbed by the load. The reflection coefficient (R_L) is a commonly used parameter for analysing microwave absorption properties of load and measuring the amount of microwave energy reflected from the load. The reflection coefficient can be determined using the following equations [248]:

$$Z_{in} = Z_0 \sqrt{\mu_r/\varepsilon_r} \tanh\left[j(2\pi f d / c)\sqrt{\mu_r \varepsilon_r}\right] \tag{23}$$

$$R_L(dB) = 20 \log \left| \frac{Z_{in} - Z_0}{Z_{in} + Z_0} \right| \tag{24}$$

Where, Z_{in} is the impedance of the sample load, Z_0 is the impedance of free space (wave guide), μ_r and ε_r are relative complex permeability and relative complex permittivity respectively, f is the operating frequency, d is the thickness of the sample and c is the velocity of light in vacuum. According to the preceding equations, the reflection coefficient is lowest and power transmission is maximum when the impedance of the load and cavity are equal to the characteristic impedance of the waveguide. The impedance of the load is influenced by various factors, including dielectric loss and magnetic loss, which are temperature dependent. This can make impedance matching challenging, especially in microwave processing of magnetic metallic materials where the magnetic loss changes with temperature and may not be known beforehand. To address this challenge adaptive matching networks known as auto tuners can adjust and match transmission line network parameters in real-time to maintain optimal impedance matching as the load impedance changes [249,250]. Optimizing P_r whether through manual or automatic impedance systems, is crucial from the early stages of research to ensure dependable laboratory results and accurate assessments of power requirements and equipment costs during scale-up. Reflected power can lead to issues such as arcing, operational instability, and irreversible damage to the microwave source. To absorb reflected power devices like circulators or isolators (three port passive MW component) are used that are connected to a separate "dummy" load, typically water circulation).

4.3. Temperature control and measurement during microwave processing

Accurate temperature readings are an essential process parameter in microwave processing of metals. Temperature readings during microwave heating may not be precise or accurate, which is one of the key objections and debate surrounding microwave efficiency as compared to conventional methods. This is because the nature of standard temperature measurement equipment poses challenges in microwave processing of metals and metal alloy materials. In addition, the temperature of the load can vary dynamically and rapidly. For instance, inserting a conventional mercury thermocouple inside a microwave applicator can disturb the field pattern, absorb some microwave and result in an electric discharge that can damage the thermocouple and lead to inaccurate temperature measurement [251,252]. An alternative to the thermocouple is the pyrometer or IR sensor, which is often used in microwave processing to measure temperature by detecting the amount of infrared radiation emitted by the object. The major disadvantage of IR sensors is that they measure the external temperature of the sample load, typically at the coldest spot due to exposure to air cooling. This characteristic can result in measurement errors, especially when the load undergoes rapid heating or has short processing times. The discrepancies in temperature readings between IR sensors and alternative methods can contribute to misunderstandings regarding microwave effects and hinder effective process control. The measuring range of IR sensors typically spans from -40 to $+2000$ °C. Relying solely on IR sensors can lead to misinterpretations, as they might register lower or higher temperatures compared to other measurement methods. This discrepancy can be attributed to environmental factors such as dust, smoke, or other particles, humidity, emissivity variations, the distance-to-target ratio, and the condition of the target surface. Fibre optic sensors provide a widely used but cost-intensive method for temperature measurement in the microwave field. Despite their precision, fibre optic sensors have limitations. They operate within a narrower range of 0–330 °C and exhibit permanent aging phenomena above 250 °C after a few hours [253]. Mechanical stress can significantly impact their sensitivity, and the use of plastics during fabrication may contribute to lower temperature resistance. However, there are specialized fibre-like single-crystal fibre for example Fiber Bragg Grating

(FBG) Sensors can typically measure temperatures around 1000 °C; GaAs-based sensors can operate in higher temperature ranges about 1200 °C and Sapphire-based sensors can withstand very high temperatures, often reaching 1600 °C can be used for high temperature applications although they may be more expensive [254,255]. Recently, a new type of thermometer called the "air-thermometer" has been developed to overcome the limitations of traditional thermometers during microwave heating [256]. The air-thermometer consists of microwave transparent quartz tubes and is based on the principle of gas expansion due to temperature change. When a gas is heated, it expands, and its pressure increases. By measuring the pressure change, the temperature of the gas can be determined.

4.4. Plasma formation and thermal runaway

The formation of plasma or hot spots and thermal runaways is one of the most critical challenges and a major topic of discussion for microwave processing of metals and metal alloy materials. Hot spots are localised areas of very high temperature that can arise mainly because of uneven heating [8]. These hotspots can induce thermal runaway, which is a self-reinforcing cycle of heating that might result in localised melting, vaporisation, or damage containment and load. In most applications, hotspots are undesirable and a sign of inefficient or improper operation, except for some applications like microwave drilling and 3D printing where hotspot caused by plasma formation is an essential part of the process. Plasma formation is undesirable for applications such as sintering, but it is more common when working with metallic powder. The plasma causes an uncontrollable temperature in the sample, affecting product quality and making the process less reproducible, as the level of plasma formation can be difficult to precisely control. On the other hand, plasma formation may be one of the key processes that leads to rapid internal heating and is therefore not a priori a negative.

4.5. Challenges in material handling, equipment design and scaling up

Another issue that arises during the microwave processing of metallic materials is their affinity for oxygen, which results in the development of oxides and changes in the electromagnetic properties of the metallic composite with temperature. Metal oxides have been found to be effective microwave absorbers because of their dielectric characteristics, which enable them to heat up more rapidly compared to metallic materials resulting to nonuniform heating and poor product quality [257–259]. However, for metals such as Ti the oxidation process led to an increase in the melting point by stabilizing their phase [260]. This can be problematic because it requires more energy to achieve the melting temperature of the material, which can prolong processing times and lead to energy wastage. To minimize oxidation during microwave processing, one technique is to fill the microwave applicator cavity with inert gases, such as argon and nitrogen. Nevertheless, it is important to select the appropriate gas composition and pressure. For example, Nitrogen is commonly used when processing non-reactive metals, while argon is preferred when working with metals such as titanium or aluminium [261].

Microwave processing of metals and metal alloy materials has been primarily limited to laboratory-scale and batch processes, with limited practical applications (metal melting) in larger-scale industrial processes [262,263]. One of the main challenges in scaling up microwave processing of metals and metal alloy materials is ensuring the same temperature profile occurs in both laboratory-scale and industrial-scale processes. Some characteristics of microwave equipment have probably impeded its broader adoption by industrial processes. A single mode applicator, for example, is constrained in size to the range of one wavelength, has a limited use in industry due to the small processing volume where the electrical field can be suitably applied, but has been very beneficial for drilling and 3D printing applications. A multimode system uses microwaves at a specific frequency to excite resonant modes
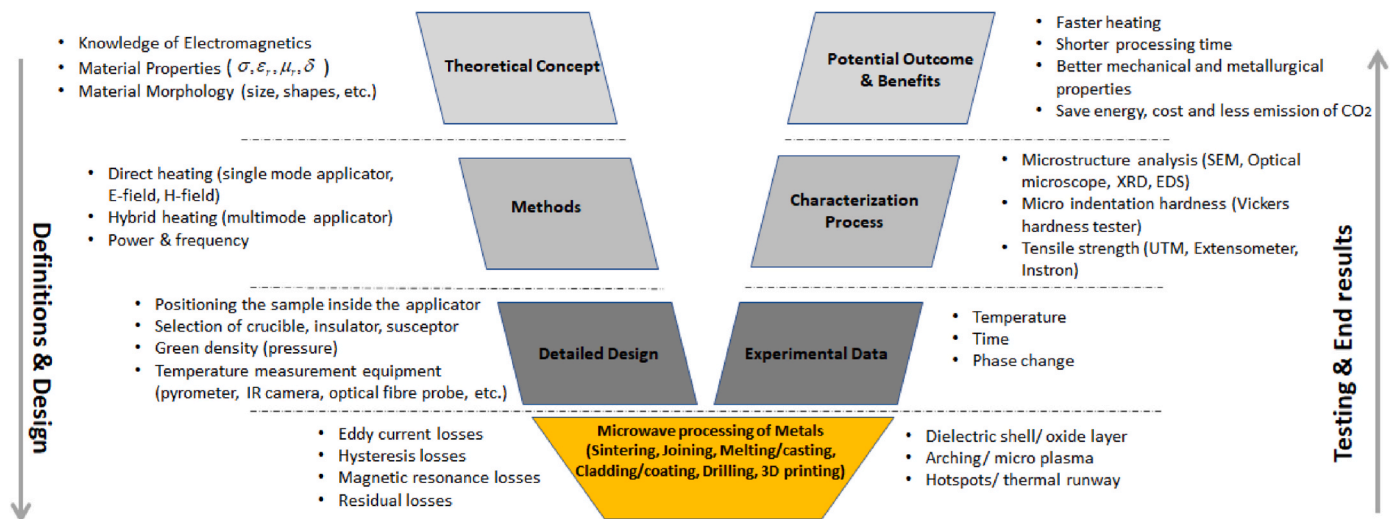
Fig. 12. Microwave processing of metal and metal alloys materials summarized in a V diagram. Source: Author.

that create areas of high and low electric fields within the cavity. Due to the non-homogeneous distribution of electromagnetic fields inside the applicator, it is very challenging to attain consistent heating across large volumes of material. Variable frequency microwaves (VFM) have been shown to have several advantages in food processing and polymer processing over traditional fixed-frequency microwaves in terms of providing time-averaged heating, uniform and selective heating over a large volume and eliminating hot spots and arcing problems [19,264, 265]. Through a coordinated effort from researchers, engineers, and manufacturers, these benefits of VFM can be realised for microwave processing of metallic materials. Scaling up from lab to large scale involves several unknowns and many uncertainties. Process simulation is a valuable tool for addressing the uncertainties and challenges associated with scaling up microwave thermal processing and can help to ensure that the process is efficient, effective, and cost-effective.

A crucial aspect in adopting new technology involves gradual scaling, moving from pilot plant testing to full-scale production. This ensures thorough evaluation and optimization for seamless integration into large-scale industrial processes. The future of microwave processing of metal-based materials presents a multifaceted landscape, involving intricate challenges and promising opportunities. Successful microwave metal processing necessitates a comprehensive understanding of various complex issues, ranging from metal-microwave interactions to efficient power delivery and stability. The overarching goal is not merely to heat or melt metals but to develop a low-cost, energy-efficient technology for processing and producing metal products. The adaptability of microwave technology to specific end-user interests while maintaining efficiency, energy efficiency, and sustainability stands out as a real strength. The ability to develop bespoke flexible systems with application-specific configurations ensures that the technology is not only versatile but also optimally suited for diverse industrial needs, making it a promising avenue for the future of sustainable and efficient metal processing. Therefore, it is important to carefully consider auxiliary materials including hybrid susceptors, containment ceramic properties and insulation. Addressing challenges to industrial implementation of this technology necessitates further research through interdisciplinary collaborations, which integrates expertise from diverse fields, allows researchers to adopt a comprehensive approach to enhance microwave technology. Numerical simulations can play a crucial role in modelling and comprehending complex processes providing insights that guide further advancements.

5. Conclusions

This review highlights selected research findings in the realm of microwave processing of metals, metal powders and alloys. In general, microwave power can be used to efficiently heat most metal powders, while it has become a viable solution for both synthesis and processing metals and metal alloy materials. Microwave processing of metals composites offers several advantages over conventional methods, including rapid heating rates, uniform heating, shorter processing times, energy savings and enhanced sustainability. Microwave processing has been successfully used to process a variety of metals and metal alloy materials, including nanoparticles, alloys, composites, and coatings and has been shown to enhance the mechanical and metallurgical properties of processed parts over and above that achievable by conventional methods. However, optimizing microwave processing of metals and metal alloy materials is dependent on complex microwave physics and the interaction with these materials, especially powders, is an area that requires further research. In particular, microwave-metal powder interactions are only partially understood and then for only a few metals and have not been investigated at all for most metals. This is an area where advances are required.

The primary factors that restrict widespread implementation of microwave processing of metallic materials in industry are explored and the challenges involved in scaling-up the technology outlined. The characteristics of microwave power and applicator equipment that focusses power onto a load (e.g fixed frequency ranges, limited flexibility in applicator geometry and managing powere reflection) are limitations hindering broader adoption in industrial processing.

In order to facilitate large-scale adoption and better control of these processes, various research directions have been proposed, such as using variable frequency microwave power, pulsed microwave power, optimization of load dimensions and scales, simulation and optimization of microwave process physics, development and employment of accurate thermal monitoring tools, and selecting appropriate susceptor and insulator materials. Finally, in the global context, where there is a growing need for more efficient and sustainable metal processing techniques that can produce high-quality products rapidly, on demand and with lower energy consumption, a schematic representation of the microwave processing of metals and metal alloy materials shown in a V diagram (Fig. 12) might be a valuable resource. This diagram provides a conceptual overview of the approach and its potential benefits.

Declaration of competing interest

The authors declare that they have no known competing financial interests or personal relationships that could have appeared to influence the work reported in this paper.

Data availability

No data was used for the research described in the article.

Acknowledgements

References

[1] International Energy Agency (2021). Global energy review 2021. 2022. https://www.iea.org/reports/industry. 05/09/2022.

[2] U.S. Energy Information Administration. "Manufacturing Energy Consumption Survey (MECS)." https://www.eia.gov/consumption/manufacturing/(accessed.

[3] Siebert JP, Hamm CM, Birkel CS. Microwave heating and spark plasma sintering as non-conventional synthesis methods to access thermoelectric and magnetic materials. Appl Phys Rev 2019;6(4).

[4] Biesuz M, Saunders T, Ke D, Reece MJ, Hu C, Grasso S. A review of electromagnetic processing of materials (EPM): heating, sintering, joining and forming. J Mater Sci Technol 2021;69:239–72.

[5] Clark DE, Sutton WH. Microwave processing of materials. Annu Rev Mater Sci 1996;26(1):299–331.

[6] Council NR. Microwave processing of materials. Washington, DC: The National Academies Press; 1994. p. 164 (in English).

[7] Bhattacharya M, Basak T. A review on the susceptor assisted microwave processing of materials. Energy 2016;97:306–38. https://doi.org/10.1016/j.energy.2015.11.034.

[8] Peng Z, Hwang J-Y. Microwave-assisted metallurgy. Int Mater Rev 2015;60(1):30–63.

[9] Oghbaei M, Mirzaee O. Microwave versus conventional sintering: a review of fundamentals, advantages and applications. J Alloys Compd 2010;494(1–2):175–89.

[10] Falciglia PP, Roccaro P, Bonanno L, De Guidi G, Vagliasindi FG, Romano S. A review on the microwave heating as a sustainable technique for environmental remediation/detoxification applications. Renew Sustain Energy Rev 2018;95:147–70.

[11] Roy R, Agrawal D, Cheng J, Gedevanishvili S. Full sintering of powdered-metal bodies in a microwave field. Nature 1999;399(6737):668–70.

[12] Cheng J, Roy R, Agrawal D. Radically different effects on materials by separated microwave electric and magnetic fields. Mater Res Innovat 2002;5(3–4):170–7.

[13] Cheng J, Roy R, Agrawal D. Experimental proof of major role of magnetic field losses in microwave heating of metal and metallic composites. J Mater Sci Lett 2001;20(17):1561–3.

[14] Porch A, Slocombe D, Edwards PP. Microwave absorption in powders of small conducting particles for heating applications. Phys Chem Chem Phys Feb 28 2013;15(8):2757–63. https://doi.org/10.1039/c2cp43310a.

[15] Thostenson E, Chou T-W. Microwave processing: fundamentals and applications. Compos Appl Sci Manuf 1999;30(9):1055–71.

[16] Saltiel C, Datta AK. Heat and mass transfer in microwave processing. Adv Heat Tran 1999;33:1–94. Elsevier.

[17] Wang B, Wu Q, Fu Y, Liu T. A review on carbon/magnetic metal composites for microwave absorption. J Mater Sci Technol 2021;86:91–109.

[18] El Khaled D, Novas N, Gazquez J, Manzano-Agugliaro F. Microwave dielectric heating: applications on metals processing. Renew Sustain Energy Rev 2018;82:2880–92.

[19] Chandrasekaran S, Ramanathan S, Basak T. Microwave material processing—a review. AIChE J 2012;58(2):330–63.

[20] Sun J, Wang W, Yue Q. Review on microwave-matter interaction fundamentals and efficient microwave-associated heating strategies. Materials Mar 25 2016;9 (4). https://doi.org/10.3390/ma9040231.

[21] Mishra RR, Sharma AK. A review of research trends in microwave processing of metal-based materials and opportunities in microwave metal casting. Crit Rev Solid State Mater Sci 2016;41(3):217–55.

[22] Meredith RJ. Engineers' handbook of industrial microwave heating (no. 25). Iet; 1998.

[23] Yoshikawa N. Fundamentals and applications of microwave heating of metals. J Microw Power Electromagn Energy 2010;44(1):4–13.

[24] Ignatenko M, Tanaka M, Sato M. Absorption of microwave energy by a spherical nonmagnetic metal particle. Jpn J Appl Phys 2009;48(6). https://doi.org/10.1143/jjap.48.067001.

[25] Rybakov K, Semenov V, Egorov S, Eremeev A, Plotnikov I, Bykov YV. Microwave heating of conductive powder materials. J Appl Phys 2006;99(2):023506.

[26] Luo J, Hunyar C, Feher L, Link G, Thumm M, Pozzo P. Theory and experiments of electromagnetic loss mechanism for microwave heating of powdered metals. Appl Phys Lett 2004;84(25):5076–8.

[27] Mondal A, Shukla A, Upadhyaya A, Agrawal D. Effect of porosity and particle size on microwave heating of copper. Sci Sinter 2010;42(2):169–82. https://doi.org/10.2298/sos1002169m.

[28] Zhang Y, Agrawal DK, Cheng J, Slawecki T. Microwave power absorption mechanism of metallic powders. IEEE Trans Microw Theor Tech 2018;66(5):2107–15.

[29] Buchelnikov V, et al. Modeling of microwave heating of metallic powders. Phys B Condens Matter 2008;403(21–22):4053–8.

[30] Gupta M, Leong EWW. Microwaves and metals. John Wiley & Sons; 2008.

[31] Roy R, Peelamedu R, Hurtt L, Cheng J, Agrawal D. Definitive experimental evidence for Microwave Effects: radically new effects of separated E and H fields, such as decrystallization of oxides in seconds. Mater Res Innovat 2016;6(3):128–40. https://doi.org/10.1007/s10019-002-0199-x.

[32] Roy R, Peelamedu R, Hurtt L, Cheng J, Agrawal D. Definitive experimental evidence for Microwave Effects: radically new effects of separated E and H fields, such as decrystallization of oxides in seconds. Mater Res Innovat 2002;6(3):128–40.

[33] Ma J, et al. Systematic study of microwave absorption, heating, and microstructure evolution of porous copper powder metal compacts. J Appl Phys 2007;101(7):074906.

[34] Roy R, Peelamedu R, Grimes C, Cheng J, Agrawal D. Major phase transformations and magnetic property changes caused by electromagnetic fields at microwave frequencies. J Mater Res 2002;17(12):3008–11.

[35] Breval E, et al. Comparison between microwave and conventional sintering of WC/Co composites. Mater Sci Eng, A 2005;391(1–2):285–95.

[36] Cao Z, Wang Z, Yoshikawa N, Taniguchi S. Microwave heating origination and rapid crystallization of PZT thin films in separated H field. J Phys Appl Phys 2008;41(9):092003.

[37] Cao Z, Yoshikawa N, Taniguchi S. Directional selectivity of microwave H field heating of Au thin films and non-doped Si plates. Mater Chem Phys 2009;117(1):14–7.

[38] Cao Z, Yoshikawa N, Taniguchi S. Microwave heating behavior of nanocrystalline Au thin films in single-mode cavity. J Mater Res 2009;24(1):268–73.

[39] Cao Z, Yoshikawa N, Taniguchi S. Microwave heating behaviors of Si substrate materials in a single-mode cavity. Mater Chem Phys 2010;124(2–3):900–3.

[40] Das S, Mukhopadhyay AK, Datta S, Basu D. Prospects of microwave processing: an overview. Bull Mater Sci 2009;32(1):1–13.

[41] Dube D, Fu M, Agrawal D, Roy R, Santra A. Rapid alloying of silicon with germanium in microwave field using single mode cavity. Mater Res Innovat 2008;12(3):119–22.

[42] Marcelo T, Mascarenhas JM, Oliveira FAC. Microwave sintering–a novel approach to powder technology. Mater Sci Forum 2010;636:946–51. Trans Tech Publ.

[43] Roy R, Fang Y, Cheng J, Agrawal DK. Decrystallizing solid crystalline titania, without melting, using microwave magnetic fields. J Am Ceram Soc 2005;88(6):1640–2.

[44] Saitou K. Microwave sintering of iron, cobalt, nickel, copper and stainless steel powders. Scripta Mater 2006;54(5):875–9. https://doi.org/10.1016/j.scriptamat.2005.11.006.

[45] Tanaka M, Kono H, Maruyama K. Selective heating mechanism of magnetic metal oxides by a microwave magnetic field. Phys Rev B 2009;79(10):104420.

[46] Ignatenko M, Tanaka M, Sato M. Absorption of microwave energy by a spherical nonmagnetic metal particle. Jpn J Appl Phys 2009;48(6R):067001.

[47] Peng Z, Hwang J-Y, Andriese M. Magnetic loss in microwave heating. APEX 2012;5(2):027304.

[48] Kato T, et al. Microwave magnetic field heating of a cobalt-based amorphous ribbon. Jpn J Appl Phys 2011;50(3R):033001.

[49] Mishra RR, Sharma AK. Microwave–material interaction phenomena: heating mechanisms, challenges and opportunities in material processing. Compos Appl Sci Manuf 2016;81:78–97. https://doi.org/10.1016/j.compositesa.2015.10.035.

[50] Amini A, Latifi M, Chaouki J. Electrification of materials processing via microwave irradiation: a review of mechanism and applications. Appl Therm Eng 2021;193:117003.

[51] Al-Shamma'a AI, Wylie SR, Lucas J, Yan JD. Atmospheric microwave plasma jet for material processing. IEEE Trans Plasma Sci 2002;30(5):1863–71.

[52] Shin DH, et al. Modification of metal surfaces by microwave plasma at atmospheric pressure. Surf Coating Technol 2007;201(9–11):4939–42.

[53] Hayashi M, Yokoyama Y, Nagata K. Effect of particle size and relative density on powdery Fe3O4 microwave heating. J Microw Power Electromagn Energy 2010;44(4):198–206.

[54] Schulz R, Folz D. Microwave and radio frequency applications. In: Proceedings of the fourth world congress on microwave and radio frequency applications, the microwave working group ltd. Maryland: Arnold; 2004.

[55] Crane C, Pantoya M, Weeks B, Saed M. The effects of particle size on microwave heating of metal and metal oxide powders. Powder Technol 2014;256:113–7.

[56] Yoshikawa N, Xie G, Cao Z, Louzguine DV. Microstructure of selectively heated (hot spot) region in Fe3O4 powder compacts by microwave irradiation. J Eur Ceram Soc 2012;32(2):419–24.

[57] Amini A, Ohno K, Maeda T, Kunitomo K. Effect of particle size and apparent density on the initial stages of temperature increase during the microwave heating of Fe3O4. Powder Technol 2018;338:101–9.

[58] Jie Z, Liu C, Huang S, Zhang G. Mechanisms of gas temperature variation of the atmospheric microwave plasma torch. J Appl Phys 2021;129(23).

[59] Sun J, Wang W, Liu Z, Ma Q, Zhao C, Ma C. Kinetic study of the pyrolysis of waste printed circuit boards subject to conventional and microwave heating. Energies 2012;5(9):3295–306.

[60] Willert-Porada M. Advances in microwave and radio frequency processing. Springer; 2006.

[61] Agrawal D. Microwave sintering of metal powders. In: Advances in powder metallurgy. Elsevier; 2013. p. 361–79.

[62] Sharma AK, Mishra RR. Role of particle size in microwave processing of metallic material systems. Mater Sci Technol 2017;34(2):123–37. https://doi.org/10.1080/02670836.2017.1412043.

[63] Khattak HK, Bianucci P, Slepkov AD. Linking plasma formation in grapes to microwave resonances of aqueous dimers. Proc Natl Acad Sci USA 2019;116(10):4000–5.

[64] Fujiwara H, Toyota S, Anggraini L, Ameyama K, Agrawal D. Microwave heating behavior of fine stainless stell powders in H-field at 2.45 GHz. In: International microwace power insitute's 44th annual symposium; 2010. p. 79–83.

[65] Yoshikawa N, Ishizuka E, Taniguchi S. Heating of metal particles in a single-mode microwave applicator. Mater Trans 2006;47(3):898–902.

[66] Gall D. Electron mean free path in elemental metals. J Appl Phys 2016;119(8).

[67] Mishra P, Upadhyaya A, Sethi G. Modeling of microwave heating of particulate metals. Metall Mater Trans B 2006;37(5):839–45. https://doi.org/10.1007/s11663-006-0066-z.

[68] Tayier W, Janasekaran S, Tai VC. Microwave hybrid heating (MHH) of Ni-based alloy powder on Ni and steel-based metals–A review on fundamentals and parameters. International Journal of Lightweight Materials and Manufacture 2022;5(1):58–73.

[69] Wong W, Gupta M. Development of metallic materials using hybrid microwave assisted rapid sintering. ASME International Mechanical Engineering Congress and Exposition 2005;42347:453–9.

[70] Balanis CA. Advanced engineering electromagnetics. John Wiley & Sons; 2012.

[71] Glasser L. Periodic tables on the world wide web. Chemistry International–Newsmagazine for IUPAC 2012;34(5):26–7.

[72] Edwards TC, Steer MB. Foundations for microstrip circuit design. John Wiley & Sons; 2016.

[73] Ashby MF, Shercliff H, Cebon D. Materials: engineering, science, processing and design. Butterworth-Heinemann; 2018.

[74] Yan P, Shen Y, Du X, Chong J. Microwave absorption properties of magnetite particles extracted from nickel slag. Materials 2020;13(9):2162.

[75] Kirby BW. Alternative crucibles for U-Mo microwave melting. Richland, WA (United States): Pacific Northwest National Lab.(PNNL); 2017.

[76] Nightingale SA. Sintering of yttria-doped zirconia ceramics in a microwave field. 1995.

[77] Bringhurst S, Andrade OM, Iskander MF. High-temperature dielectric properties measurements of ceramics. MRS Online Proc Libr 1992;269.

[78] Ashby MF. "Materials selection in mechanical design. Elsevier Science 2005;141:1741–3.

[79] Chen L-F, Ong CK, Neo C, Varadan VV, Varadan VK. Microwave electronics: measurement and materials characterization. John Wiley & Sons; 2004.

[80] Varadan VV, Hollinger RD, Ghodgaonkar DK, Varadan VK. Free-space, broadband measurements of high-temperature, complex dielectric properties at microwave frequencies. IEEE Trans Instrum Meas 1991;40(5):842–6.

[81] Ling W, Xa Q, Yan L, Wang C, Cao M, Liu L. Preparation, morphology and dielectric properties of nano-TiC/polyimide composite films. Polym Polym Compos 2014;22(2):123–8.

[82] Lam SS, et al. Microwave vacuum pyrolysis of waste plastic and used cooking oil for simultaneous waste reduction and sustainable energy conversion: recovery of cleaner liquid fuel and techno-economic analysis. Renew Sustain Energy Rev 2019;115:109359.

[83] Xu Gf, Olorunyolemi T, Carmel Y, Lloyd IK, Wilson OC. Design and construction of insulation configuration for ultra-high-temperature microwave processing of ceramics. J Am Ceram Soc 2003;86(12):2082–6.

[84] Gupta M, Wong W. Enhancing overall mechanical performance of metallic materials using two-directional microwave assisted rapid sintering. Scripta Mater 2005;52(6):479–83.

[85] Xu F, Li Y, Hu X, Niu Y, Zhao J, Zhang Z. In situ investigation of metal's microwave sintering. Mater Lett 2012;67(1):162–4.

[86] Leparoux S, Vaucher S, Beffort O. Assessment of microwave heating for sintering of al/sic and for in-situ synthesis of tic. Adv Eng Mater 2003;5(6):449–53.

[87] Venkateswarlu K, Saurabh S, Rajinikanth V, Sahu RK, Ray AK. Synthesis of TiN reinforced aluminium metal matrix composites through microwave sintering. J Mater Eng Perform 2010;19:231–6.

[88] Zhu H, Guo G, Cui T, Huang J, Li J, Xie Z. In situ aluminum matrix composites fabricated from Al–Ni2O3 system through microwave synthesis. Mater Chem Phys 2015;153:333–7.

[89] Ghasali E, Yazdani-rad R, Asadian K, Ebadzadeh T. Production of Al-SiC-TiC hybrid composites using pure and 1056 aluminum powders prepared through microwave and conventional heating methods. J Alloys Compd 2017;690:512–8.

[90] Saheb N. Spark plasma and microwave sintering of Al6061 and Al2124 alloys. Int J Miner Metall Mater 2013;20:152–9.

[91] Olaniran O, Akinwande AA, Adediran A, Jen T-C. Microstructural characterization and properties of aluminium 7075/Mo prepared by microwave sintering for high-strength application. Advances in materials and processing technologies. 2022. p. 1–14.

[92] Anklekar R, Agrawal D, Roy R. Microwave sintering and mechanical properties of PM copper steel. Powder Metall 2001;44(4):355–62.

[93] Padmavathi C, Upadhyaya A, Agrawal D. Effect of microwave and conventional heating on sintering behavior and properties of Al–Mg–Si–Cu alloy. Mater Chem Phys 2011;130(1–2):449–57.

[94] Annamalai R, Upadhyaya A, Agrawal D. An investigation on microwave sintering of Fe, Fe–Cu and Fe–Cu–C alloys. Bull Mater Sci 2013;36:447–56.

[95] Mahmoud M, Link G, Jelonnek J, Thumm M. Investigation of mm-wave sintering of metal powder compacts using in-situ dilatometry and electrical resistivity measurements. EPJ web of conferences, vol. 149. EDP Sciences; 2017, 02007.

[96] Takayama S, Saito Y, Sato M, Nagasaka T, Muroga T, Ninomiya Y. Sintering behavior of metal powders involving microwave-enhanced chemical reaction. Jpn J Appl Phys 2006;45(3R):1816.

[97] Demirskyi D, Agrawal D, Ragulya A. Neck formation between copper spherical particles under single-mode and multimode microwave sintering. Mater Sci Eng, A 2010;527(7–8):2142–5.

[98] Demirskyi D, Agrawal D, Ragulya A. Densification kinetics of powdered copper under single-mode and multimode microwave sintering. Mater Lett 2010;64(13):1433–6. https://doi.org/10.1016/j.matlet.2010.03.047.

[99] Demirskyi D, Agrawal D, Ragulya A. Neck growth kinetics during microwave sintering of copper. Scripta Mater 2010;62(8):552–5. https://doi.org/10.1016/j.scriptamat.2009.12.036.

[100] Ma J, et al. Systematic study of microwave absorption, heating, and microstructure evolution of porous copper powder metal compacts. J Appl Phys 2007;101(7). https://doi.org/10.1063/1.2713087.

[101] Demirskyi D, Agrawal D, Ragulya A. A scaling law study of the initial stage of microwave sintering of iron spheres. Scripta Mater 2012;66(6):323–6.

[102] Roy R, Agrawal DK, Cheng J. Process for sintering powder metal components. Google Patents; 2001.

[103] Nadjafi Maryam Negari A, Mamoory R, Simchi A, Ehsani N. Determination of the physical and mechanical properties of iron-based powder materials produced by microwave sintering. Powder Metall Met Ceram 2007;46:423–8.

[104] Anklekar R, Bauer K, Agrawal DK, Roy R. Improved mechanical properties and microstructural development of microwave sintered copper and nickel steel PM parts. Powder Metall 2005;48(1):39–46.

[105] Veronesi P, Leonelli C, Bassoli E, Gatto A, Iuliano L. Microwave assisted sintering of SLS green metal parts. nd. In: proc. of Sintering 2003; 2003. nd-nd.

[106] Zhou C, Yi J, Luo S, Peng Y, Li L, Chen G. Effect of heating rate on the microwave sintered W–Ni–Fe heavy alloys. J Alloys Compd 2009;482(1–2):L6–8.

[107] Panda SS, Singh V, Upadhyaya A, Agrawal D. Sintering response of austenitic (316L) and ferritic (434L) stainless steel consolidated in conventional and microwave furnaces. Scripta Mater 2006;54(12):2179–83. https://doi.org/10.1016/j.scriptamat.2006.02.034.

[108] Nagaraju K, Kumaran S, Rao TS. Microwave sintering of 316L stainless steel: influence of sintering temperature and time. Mater Today Proc 2020;27:2066–71.

[109] Veera Venkata Nagaraju K, Kumaran S, Srinivasa Rao T. Microwave sintering response of different grade stainless steels and its influence on metallurgical properties. Powder Metall 2021:1–14. https://doi.org/10.1080/00325899.2021.1981656.

[110] Venkata Nagaraju KV, Kumaran S, Rao TS. Densification kinetics of P/M austenitic (316L) stainless steels processed by rapid microwave hybrid heating method at various conditions. Advances in materials and processing technologies. 2021. p. 1–14. https://doi.org/10.1080/2374068x.2021.1970993.

[111] Z. Cheng, J. Shi, T. Barriere, J. Gelin, and B. Liu, "Manuscript refereed by professor fátima barreiros (Polytechnic institute of leiria, Portugal): microwave sintering of stainless steel powder with high efficiency and gradient in mechanic properties," in *European Congress and Exhibition on powder metallurgy. European PM conference proceedings*, 2015: the European powder metallurgy association, p. 1.

[112] Jun M, Huiping T, Aijun L. Microwave sintering of 316L stainless steel fiber felt. Rare Met Mater Eng 2017;46(9):2379–83.

[113] Raja Annamalai A, Upadhyaya A, Agrawal D. Effect of heating mode and electrochemical response on austenitic and ferritic stainless steels. Can Metall Q 2015;54(2):142–8.

[114] Ertugrul O, Park HS, Onel K, Willert-Porada M. Effect of particle size and heating rate in microwave sintering of 316L stainless steel. Powder Technol 2014;253:703–9. https://doi.org/10.1016/j.powtec.2013.12.043.

[115] Kennedy S, Kumaran S, Srinivasa Rao T. Microstructure and mechanical properties of microwave sintered austenitic stainless steel. Trans Indian Inst Met 2011;64:85–7.

[116] Demirskyi D, Agrawal D, Ragulya A. Neck growth kinetics during microwave sintering of nickel powder. J Alloys Compd 2011;509(5):1790–5.

[117] Yadoji P, Peelamedu R, Agrawal D, Roy R. Microwave sintering of Ni–Zn ferrites: comparison with conventional sintering. Mater Sci Eng, B 2003;98(3):269–78.

[118] Peelamedu R, Grimes C, Agrawal D, Roy R, Yadoji P. Ultralow dielectric constant nickel–zinc ferrites using microwave sintering. J Mater Res 2003;18:2292–5.

[119] Penchal Reddy M, et al. Microwave sintering of nickel ferrite nanoparticles processed via sol–gel method. J Sol Gel Sci Technol 2014;70:400–4.

[120] Hoyos J, Zabotto F, Garcia D, Kiminami R. Microwave sintering of nickel ferrite synthesized by the Pechini method. Cerâmica 2013;59:360–5.

[121] Upadhyaya A, Tiwari S, Mishra P. Microwave sintering of W–Ni–Fe alloy. Scripta Mater 2007;56(1):5–8.

[122] Mondal A, Agrawal D, Upadhyaya A. Microwave sintering of refractory metals/alloys: W, Mo, Re, W-Cu, W-Ni-Cu and W-Ni-Fe alloys. J Microw Power Electromagn Energy 2010;44(1):28–44.

[123] Thirunavukkarasu M, et al. Optimal parameters of microwave sintering process on nickel based composite. Mater Today Proc 2022;66:653–7.

[124] Rybakov K, Buyanova M. Microwave resonant sintering of powder metals. Scripta Mater 2018;149:108–11.

[125] Charmond S, Bouvard D, Carry C. Microwave sintering: attempts to sinter a fine nickel powder in a microwave single-mode cavity. In: European congress and exhibition on powder metallurgy. European PM conference proceedings. The European Powder Metallurgy Association; 2009. p. 1.

[126] Prabhu G, Chakraborty A, Sarma B. Microwave sintering of tungsten. Int J Refract Metals Hard Mater 2009;27(3):545–8.

[127] Wang K, et al. The study on the microwave sintering of tungsten at relatively low temperature. J Nucl Mater 2012;431(1–3):206–11.

[128] Bao R, Yi J. Densification and alloying of microwave sintering WC–8 wt.% Co composites. Int J Refract Metals Hard Mater 2014;43:269–75.

[129] Wong WE, Gupta M. Simultaneously improving strength and ductility of magnesium using nano-size SiC particulates and microwaves. Adv Eng Mater 2006;8(8):735–40.

[130] Zhong X, Wong W, Gupta M. Enhancing strength and ductility of magnesium by integrating it with aluminum nanoparticles. Acta Mater 2007;55(18):6338–44.

[131] Sankaranarayanan S, Habibi M, Jayalakshmi S, Jia Ai K, Almajid A, Gupta M. Nano-AlN particle reinforced Mg composites: microstructural and mechanical properties. Mater Sci Technol 2015;31(9):1122–31.

[132] Wong WLE, Gupta M. Using microwave energy to synthesize light weight/energy saving magnesium based materials: a review. Technologies 2015;3(1):1–18.

[133] Leong Eugene WW, Gupta M. Characteristics of aluminum and magnesium based nanocomposites processed using hybrid microwave sintering. J Microw Power Electromagn Energy 2010;44(1):14–27.

[134] Wong WLE, Gupta M. Improving overall mechanical performance of magnesium using nano-alumina reinforcement and energy efficient microwave assisted processing route. Adv Eng Mater 2007;9(10):902–9.

[135] Sethi G, Upadhyaya A, Agrawal D. Microwave and conventional sintering of premixed and prealloyed Cu-12Sn bronze. Sci Sinter 2003;35(2):49–65.

[136] Manière C, Saccardo E, Lee G, McKittrick J, Molinari A, Olevsky EA. Swelling negation during sintering of sterling silver: an experimental and theoretical approach. Results Phys 2018;11:79–84.

[137] Olmos L, Bouvard D, Salvo L, Bellet D, Di Michiel M. Characterization of the swelling during sintering of uniaxially pressed copper powders by in situ X-ray microtomography. J Mater Sci 2014;49:4225–35.

[138] Sato M, Fukusima H, Ozeki F, Hayasi T, Saito Y, Takayama S. Experimental investigation of mechanism of microwave heating in powder metals. In: Infrared and millimeter waves, conference digest of the 2004 joint 29th international conference on 2004 and 12th international conference on terahertz electronics, 2004. IEEE; 2004. p. 831–2.

[139] Buchelnikov V, et al. Heating of metallic powders by microwaves: experiment and theory. J Appl Phys 2008;104(11):113505.

[140] Luo S, Yan M, Schaffer G, Qian M. Sintering of titanium in vacuum by microwave radiation. Metall Mater Trans 2011;42:2466–74.

[141] Luo SD, Qian M, Imam MA. Microwave sintering of titanium and titanium alloys. In: Titanium powder metallurgy. Elsevier; 2015. p. 237–51.

[142] Raynova S, Imam M, Yang F, Bolzoni L. Hybrid microwave sintering of blended elemental Ti alloys. J Manuf Process 2019;39:52–7.

[143] Imam MA, Feng J, Rock BY, Fliflet AW. Processing of titanium and its alloys by microwave energy. Adv Mater Res 2014;1019:11–8. Trans Tech Publ.

[144] Luo S, Qian M. Microwave processing of titanium and titanium alloys for structural, biomedical and shape memory applications: current status and challenges. Mater Manuf Process 2018;33(1):35–49.

[145] Singh D, Rana A, Sharma P, Pandey PM, Kalyanasundaram D. Microwave sintering of Ti6Al4V: optimization of processing parameters for maximal tensile strength and minimal pore size. Metals 2018;8(12):1086.

[146] Vasudevan N, Ahamed NNN, Pavithra B, Aravindhan A, Shanmugavel BP. Effect of Ni addition on the densification of TiC: a comparative study of conventional and microwave sintering. Int J Refract Metals Hard Mater 2020;87:105165.

[147] Hong M, Zou J, Chen Z-G. Synthesis of thermoelectric materials. In: Thermoelectricity and advanced thermoelectric materials. Elsevier; 2021. p. 73–103.

[148] González-Barrios MM, et al. Microwave-assisted synthesis of thermoelectric oxides and chalcogenides. Ceram Int 2022;48(9):12331–41.

[149] Yong C, et al. Microwave synthesis and excellent thermoelectric performances of Yb-filled CoSb3 skutterudites. Mater Res Bull 2023;162:112187.

[150] Birkel CS, et al. Rapid microwave preparation of thermoelectric TiNiSn and TiCoSb half-Heusler compounds. Chem Mater 2012;24(13):2558–65.

[151] Agrawal D. Microwave sintering, brazing and melting of metallic materials. Sohn International Symposium; Advanced Processing of Metals and Materials Volume 4: New, Improved and Existing Technologies: Non-Ferrous Materials Extraction and Processing 2006;4:183–92.

[152] Ripley EB, et al. Current advances in microwave processing of metals, and related emerging technologies. American Institute of Chemical Engineers; 2004.

[153] Ripley EB, Oberhaus JA. WWWeb Search Power Page-Melting and Heat Treating Metals Using Microwave Heating-The potential of microwave metal processing techniques for a wide variety of metals and alloys is. Industrial heating 2005;72 (5):65–70.

[154] Chandrasekaran S, Basak T, Ramanathan S. Experimental and theoretical investigation on microwave melting of metals. J Mater Process Technol 2011;211 (3):482–7. https://doi.org/10.1016/j.jmatprotec.2010.11.001.

[155] Mishra RR, Sharma AK. On melting characteristics of bulk Al-7039 alloy during in-situ microwave casting. Appl Therm Eng 2017;111:660–75.

[156] Mishra RR, Sharma AK. Microwave heating characteristics of bulk metallic materials. J Mater Sci 2018;53(24):16567–84.

[157] Xu L, Srinivasakannan C, Peng J, Guo S, Xia H. Study on characteristics of microwave melting of copper powder. J Alloys Compd 2017;701:236–43. https://doi.org/10.1016/j.jallcom.2017.01.097.

[158] Lingappa MS, Srinath M, Amarendra H. Microstructural and mechanical investigation of aluminium alloy (Al 1050) melted by microwave hybrid heating. Mater Res Express 2017;4(7):076504.

[159] Sun X, Hwang J-Y, Huang X, Li B, Shi S. Effects of microwave on molten metals with low melting temperatures. J Miner Mater Char Eng 2005;4(2):107–12.

[160] Huhtamäki T, Tian X, Korhonen JT, Ras RH. Surface-wetting characterization using contact-angle measurements. Nat Protoc 2018;13(7):1521–38.

[161] Eustathopoulos N. Wetting by liquid metals—application in materials processing: the contribution of the grenoble group. Metals 2015;5(1):350–70.

[162] Durov A, Naidich Y, Kostyuk B. Investigation of interaction of metal melts and zirconia. J Mater Sci 2005;40.

[163] Nikolopoulos P, Sotiropoulou D. Wettability between zirconia ceramics and the liquid metals copper, nickel and cobalt. J Mater Sci Lett 1987;6:1429–30.

[164] Leon C, Drew R. The influence of nickel coating on the wettability of aluminum on ceramics. Compos Appl Sci Manuf 2002;33(10):1429–32.

[165] Trontelj M, Kolar D. Wetting of aluminum nitride by nickel alloys. J Am Ceram Soc 1978;61(5-6):204–7.

[166] Liu G, Muolo M, Valenza F, Passerone A. Survey on wetting of SiC by molten metals. Ceram Int 2010;36(4):1177–88.

[167] Ueki M, Naka M, Okamoto I. Wettability of some metals against zirconia ceramics. J Mater Sci Lett 1986;5:1261–2.

[168] Lin Q, Tan K, Wang L, Sui R. Wetting of YSZ by molten Sn–8Zr, Sn–4Zr–4Ti, and Sn–8Ti alloys at 800–900° C. Ceram Int 2022;48(1):373–80.

[169] Lin C-C, Chen R-B, Shiue R-K. A wettability study of Cu/Sn/Ti active braze alloys on alumina. J Mater Sci 2001;36:2145–50.

[170] Tomsia A, Pask J, Loehman R. Joining nitride ceramics. In: Proceedings of the international forum on structural ceramics joining: ceramic engineering and science proceedings. Wiley Online Library; 1989. p. 1631–54.

[171] So KP, et al. SiC formation on carbon nanotube surface for improving wettability with aluminum. Compos Sci Technol 2013;74:6–13.

[172] Li J-G. Wetting of ceramic materials by liquid silicon, aluminium and metallic melts containing titanium and other reactive elements: a review. Ceram Int 1994; 20(6):391–412.

[173] Sobczak N. Effects of titanium on wettability and interfaces in aluminium/ceramic systems. Characterization & control of interfaces for high quality advanced materials 2005;146:83–91.

[174] Nicholas M. Ceramic-metal interfaces. Surfaces and Interfaces of Ceramic Materials 1989:393–417.

[175] Chen J, Gu M, Pan F. Reactive wetting of a metal/ceramic system. J Mater Res 2002;17(4):911–7.

[176] Rhee S. Wetting of AlN and TiC by liquid Ag and liquid Cu. J Am Ceram Soc 1970; 53(12):639–41.

[177] Singh M, Shpargel T, Asthana R. Brazing of stainless steel to yttria-stabilized zirconia using gold-based brazes for solid oxide fuel cell applications. Int J Appl Ceram Technol 2007;4(2):119–33.

[178] Yuan Z, Huang W, Mukai K. Wettability and reactivity of molten silicon with various substrates. Appl Phys A 2004;78:617–22.

[179] Taranets NY, Naidich YV. Wettability of aluminum nitride by molten metals. Powder Metall Met Ceram 1996;35(5–6):282–5.

[180] Liu A, Li B, Sui Y, Guo J. Wettability of titanium on calcia-stabilized zirconia in electromagnetic field. Mater Lett 2012;89:299–301.

[181] Zhu J, Kamiya A, Yamada T, Shi W, Naganuma K, Mukai K. Surface tension, wettability and reactivity of molten titanium in Ti/yttria-stabilized zirconia system. Mater Sci Eng, A 2002;327(2):117–27.

[182] Karasangabo A, Bernhard C. Investigation of alumina wetting by Fe–Ti, Fe–P and Fe–Ti–P alloys. J Adhes Sci Technol 2012;26(8–9):1141–56.

[183] Mattia D, Desmaison-Brut M, Tétard D, Desmaison J. Wetting of HIP AlN-TiB2 ceramic composites by liquid metals and alloys. J Eur Ceram Soc 2005;25(10):1797–803.

[184] Contreras A, Leon C, Drew R, Bedolla E. Wettability and spreading kinetics of Al and Mg on TiC. Scripta Mater 2003;48(12):1625–30.

[185] Ploetz S, Nowak R, Lohmueller A, Sobczak N, Singer RF. Wettability of low weight borides by commercial aluminum alloys– a basis for metal matrix composite fabrication. Adv Eng Mater 2016;18(11):1884–8.

[186] Benko E. Wettability studies of cubic boron nitride by silver-titanium. Ceram Int 1995;21(5):303–7.

[187] Gupta D, Sharma AK. Microwave cladding: a new approach in surface engineering. J Manuf Process 2014;16(2):176–82.

[188] Somani N, Kumar K, Gupta N. Review on microwave cladding: a new approach. In: Advances in materials processing: select proceedings of ICFMMP 2019. Springer; 2020. p. 77–90.

[189] Loharkar PK, Ingle A, Jhavar S. Parametric review of microwave-based materials processing and its applications. J Mater Res Technol 2019;8(3):3306–26.

[190] Gupta D, Sharma AK. Development and microstructural characterization of microwave cladding on austenitic stainless steel. Surf Coating Technol 2011;205 (21–22):5147–55.

[191] Gupta D, Bhovi PM, Sharma AK, Dutta S. Development and characterization of microwave composite cladding. J Manuf Process 2012;14(3):243–9.

[192] Sharma AK, Gupta D. On microstructure and flexural strength of metal–ceramic composite cladding developed through microwave heating. Appl Surf Sci 2012; 258(15):5583–92.

[193] Bansal A, Zafar S, Sharma AK. Microstructure and abrasive wear performance of Ni-WC composite microwave clad. J Mater Eng Perform 2015;24:3708–16.

[194] Bansal S, Mago J, Gupta D, Jain V. Microwave cladding of NiCrSiC-5Al2O3 on austenitic stainless steel to improve cavitation erosion resistance. Surf Topogr Metrol Prop 2021;9(3):035036.

[195] Bansal S, Mago J, Gupta D, Jain V. Parametric optimization and analysis of cavitation erosion behavior of Ni-based+ 10WC microwave processed composite clad using Taguchi approach. Surf Topogr Metrol Prop 2021;9(1):015011.

[196] Bansal S, Gupta D, Jain V. Surface modification OF SS-316 to enhance cavitation resistance through composite microwave clads. Surf Rev Lett 2021:2141004.

[197] Singh B, Zafar S. Understanding temperature characteristics during microwave cladding through process modeling and experimental investigation. CIRP Journal of Manufacturing Science and Technology 2022;37:401–13.

[198] Zafar S, Bansal A, Sharma A, Arora N, Ramesh C. Dry erosion wear performance of Inconel 718 microwave clad. Surf Eng 2014;30(11):852–9.

[199] Zafar S, Sharma AK. Development and characterisations of WC–12Co microwave clad. Mater Char 2014;96:241–8.

[200] Zafar S, Sharma AK. On friction and wear behavior of WC-12Co microwave clad. Tribol Trans 2015;58(4):584–91.

[201] Zafar S, Sharma AK. Dry sliding wear performance of nanostructured WC–12Co deposited through microwave cladding. Tribol Int 2015;91:14–22.

[202] Zafar S, Sharma AK. Abrasive and erosive wear behaviour of nanometric WC–12Co microwave clads. Wear 2016;346:29–45.

[203] Prasad CD, Lingappa MS, Joladarashi S, Ramesh M, Sachin B. Characterization and sliding wear behavior of CoMoCrSi+ Flyash composite cladding processed by microwave irradiation. Mater Today Proc 2021;46:2387–91.

[204] Grewal H, Nair R, Arora H. Complex concentrated alloy bimodal composite claddings with enhanced cavitation erosion resistance. Surf Coating Technol 2020;392:125751.

[205] Hebbale AM, Srinath M. Microstructural investigation of Ni based cladding developed on austenitic SS-304 through microwave irradiation. J Mater Res Technol 2016;5(4):293–301.

[206] Hasan M, Zhao J, Jiang Z. A review of modern advancements in micro drilling techniques. J Manuf Process 2017;29:343–75.

[207] Jerby E, Dikhtyar V, Aktushev O, Grosglick U. The microwave drill. Science 2002; 298(5593):587–9.

[208] Alpert Y, Jerby E. Coupled thermal-electromagnetic model for microwave heating of temperature-dependent dielectric media. IEEE Trans Plasma Sci 1999;27(2): 555–62.

[209] Eshet Y, Mann RR, Anaton A, Yacoby T, Gefen A, Jerby E. Microwave drilling of bones. IEEE Trans Biomed Eng 2006;53(6):1174–82.

[210] Jerby E, et al. Microwave drill applications for concrete, glass and silicon. In: Proc. 4th world congress microw. Radio-frequency applications. New York: American Institute of Chemical Engineers; 2004. p. 4–7.

[211] Jerby E, Thompson AM. Microwave drilling of ceramic thermal-barrier coatings. J Am Ceram Soc 2004;87(2):308–10.

[212] Jerby E, Dikhtyar V. Drilling into hard non-conductive materials by localized microwave radiation. In: Advances in microwave and radio frequency processing: report from the 8th international conference on microwave and high frequency heating held in bayreuth, Germany, september 3–7, 2001. Springer; 2006. p. 687–94.

[213] Meir Y, Jerby E. Localized rapid heating by low-power solid-state microwave drill. IEEE Trans Microw Theor Tech 2012;60(8):2665–72.

[214] George TJ, Sharma AK, Kumar P. A feasibility study on drilling of metals through microwave heating. i-manager's Journal on Mechanical Engineering 2012;2(2): 1–6.

[215] Lautre NK, Sharma AK, Kumar P, Das S. Performance of different drill bits in microwave assisted drilling. International Journal of Mechanical Engineering and Robotics Research 2014;1(1):22–9.

[216] Singh A, Sharma AK. On microwave drilling of metal-based materials at 2.45 GHz. Appl Phys A 2020;126(10):822.

[217] Zhang Y, Feng D, He Z-y, Chen X-c. Progress in joining ceramics to metals. J Iron Steel Res Int 2006;13(2):1–5.

[218] Samyal R, Bagha AK, Bedi R. Microwave joining of similar/dissimilar metals and its characterizations: a review. Mater Today Proc 2020;26:423–33.

[219] Nandwani S, Vardhan S, Bagha AK. A literature review on the exposure time of microwave based welding of different materials. Mater Today Proc 2020;27: 2526–8.

[220] Handa V, Goyal P, Sehgal S. Review of joining inconel alloys through microwave hybrid heating and other techniques. Mater Today Proc 2020;28:1355–8.

[221] Naik TP, Singh I, Sharma AK. Processing of polymer matrix composites using microwave energy: a review. Compos Appl Sci Manuf 2022:106870.

[222] Srinath M, Sharma AK, Kumar P. Investigation on microstructural and mechanical properties of microwave processed dissimilar joints. J Manuf Process 2011;13(2): 141–6.

[223] Srinath M, Sharma AK, Kumar P. A new approach to joining of bulk copper using microwave energy. Mater Des 2011;32(5):2685–94.

[224] Srinath M, Sharma AK, Kumar P. A novel route for joining of austenitic stainless steel (SS-316) using microwave energy. Proc IME B J Eng Manufact 2011;225(7): 1083–91.

[225] Badiger RI, Narendranath S, Srinath M. Joining of Inconel-625 alloy through microwave hybrid heating and its characterization. J Manuf Process 2015;18: 117–23.

[226] Badiger RI, Narendranath S, Srinath M. Microstructure and mechanical properties of Inconel-625 welded joint developed through microwave hybrid heating. Proc IME B J Eng Manufact 2018;232(14):2462–77.

[227] Bansal A, Sharma AK, Kumar P, Das S. Characterization of bulk stainless steel joints developed through microwave hybrid heating. Mater Char 2014;91:34–41.

[228] Bagha L, Sehgal S, Thakur A, Kumar H. Effects of powder size of interface material on selective hybrid carbon microwave joining of SS304–SS304. J Manuf Process 2017;25:290–5.

[229] Gamit D, Mishra RR, Sharma AK. Joining of mild steel pipes using microwave hybrid heating at 2.45 GHz and joint characterization. J Manuf Process 2017;27: 158–68.

[230] Pal M, Sehgal S, Kumar H, Singh AP. Manufacturing of joints of stainless steels through microwave hybrid heating. Mater Today Proc 2018;5(14):28149–54.

[231] Kumar A, Sehgal S, Singh S, Bagha AK. Joining of SS304-SS316 through novel microwave hybrid heating technique without filler material. Mater Today Proc 2020;26:2502–5.

[232] Somani N, Singh N, Gupta NK. Joining and characterization of SS-430 using microwave hybrid heating technique. J Eng Des Technol 2021;19(6):1344–57.

[233] Frazier WE. Metal additive manufacturing: a review. J Mater Eng Perform 2014; 23:1917–28.

[234] Jerby E, et al. Stepwise consolidation of metal powder by localized microwaves for additive manufacturing of 3D structures. In: 14th Intl Conf microwave and high frequency heating; 2013. p. 345–8.

[235] Fugenfirov M, Meir Y, Shelef A, Nerovny Y, Aharoni E, Jerby E. Incremental solidification (toward 3D-printing) of magnetically-confined metal-powder by localized microwave heating. COMPEL-The international journal for computation and mathematics in electrical and electronic engineering 2018;37(6):1918–32.

[236] Shelef A, Jerby E. Incremental solidification (toward 3D-printing) of metal powders by transistor-based microwave applicator. Mater Des 2020;185:108234.

[237] Shoshani Y, Weinstein T, Barkay Z, Jerby E. Sequential solidification of metal powder by a scanning microwave applicator. Materials 2023;16(3):1136.

[238] Mostafaei A, et al. Binder jet 3D printing—process parameters, materials, properties, modeling, and challenges. Prog Mater Sci 2021;119:100707.

[239] Singh D, Garg B, Pandey PM, Kalyanasundaram D. Design and development of 3D printing assisted microwave sintering of elbow implant with biomechanical properties similar tohuman elbow. Rapid Prototyp J 2022;28(2):390–403.

[240] Salehi M, Maleksaeedi S, Nai MLS, Gupta M. Towards additive manufacturing of magnesium alloys through integration of binderless 3D printing and rapid microwave sintering. Addit Manuf 2019;29:100790.

[241] Salehi M, Seet HL, Gupta M, Farnoush H, Maleksaeedi S, Nai MLS. Rapid densification of additive manufactured magnesium alloys via microwave sintering. Addit Manuf 2021;37:101655.

[242] Tarafder S, Balla VK, Davies NM, Bandyopadhyay A, Bose S. Microwave-sintered 3D printed tricalcium phosphate scaffolds for bone tissue engineering. Journal of tissue engineering and regenerative medicine 2013;7(8):631–41.

[243] Tarafder S, Dernell WS, Bandyopadhyay A, Bose S. SrO-and MgO-doped microwave sintered 3D printed tricalcium phosphate scaffolds: mechanical properties and in vivo osteogenesis in a rabbit model. J Biomed Mater Res B Appl Biomater 2015;103(3):679–90.

[244] Li N, Link G, Engler M, Jelonnek J. Small-size coaxial resonant applicator for microwave heating assisted additive manufacturing. IEEE Trans Microw Theor Tech 2021;69(11):4631–8.

[245] Li N, Link G, Jelonnek J. 3D microwave printing temperature control of continuous carbon fiber reinforced composites. Compos Sci Technol 2020;187: 107939.

[246] Li N, Link G, Jelonnek J. Rapid 3D microwave printing of continuous carbon fiber reinforced plastics. CIRP Annals 2020;69(1):221–4.

[247] Radoiu M, Mello A. Technical advances, barriers, and solutions in microwave—assisted technology for industrial processing. Chem Eng Res Des 2022;181:331–42.

[248] Pozar DM. Microwave engineering. John wiley & sons; 2011.

[249] Yussuf A, Sbarski I, Hayes J, Solomon M, Tran N. Microwave welding of polymeric-microfluidic devices. J Micromech Microeng 2005;15(9):1692.

[250] Jerby E, Nerovny Y, Meir Y, Korin O, Peleg R, Shamir Y. A silent microwave drill for deep holes in concrete. IEEE Trans Microw Theor Tech 2017;66(1):522–9.

[251] Bartoli M, Frediani M, Briens C, Berruti F, Rosi L. An overview of temperature issues in microwave-assisted pyrolysis. Processes 2019;7(10):658.

[252] Pert E, et al. Temperature measurements during microwave processing: the significance of thermocouple effects. J Am Ceram Soc 2001;84(9):1981–6.

[253] Nüchter M, Ondruschka B, Bonrath W, Gum A. Microwave assisted synthesis–a critical technology overview. Green Chem 2004;6(3):128–41.

[254] Ma S, et al. Optical fiber sensors for high-temperature monitoring: a review. Sensors 2022;22(15):5722.

[255] Li Y, et al. Ultra-high-temperature sensing using fiber grating sensor and demodulation method based on support vector regression optimized by a genetic algorithm. Opt Express 2023;31(3):3401–14.

[256] Farag S, Chaouki J. A modified microwave thermo-gravimetric-analyzer for kinetic purposes. Appl Therm Eng 2015;75:65–72.

[257] Hou T, et al. A review of metal oxide-related microwave absorbing materials from the dimension and morphology perspective. J Mater Sci Mater Electron 2019;30: 10961–84.

[258] Peng Z, Hwang J-Y, Andriese M, Zhang Y, Li G, Jiang T. Microwave power absorption characteristics of iron oxides. Characterization of minerals, metals, and materials 2015 2016:299–305.

[259] Peng Z, Hwang J-Y, Park C-L, Kim B-G, Andriese M, Wang X. Microwave permittivity, permeability, and absorption capability of ferric oxide. ISIJ Int 2012; 52(9):1535–8.

[260] Yang X, Gao F, Tang F, Hao X, Li Z. Effect of surface oxides on the melting and solidification of 316L stainless steel powder for additive manufacturing. Metall Mater Trans 2021;52:4518–32.

[261] Sames WJ, List F, Pannala S, Dehoff RR, Babu SS. The metallurgy and processing science of metal additive manufacturing. Int Mater Rev 2016;61(5):315–60.

[262] Microwave Chemical Co Ltd. Accelerating the commercialization of energy-saving rare metal refining technology with microwave heating - national Institutes for Quantum Science and Technology and Microwave Chemical Co. Ltd; 2023. signed on joint research and development agreement for the technology demonstration, https://mwcc.jp/en/news_press/220117/. [Accessed 6 March 2023].

[263] Awida MH, Shah N, Warren B, Ripley E, Fathy AE. Modeling of an industrial microwave furnace for metal casting applications. In: 2008 IEEE MTT-S international microwave symposium digest. IEEE; 2008. p. 221–4.

[264] Ku H, Siu F, Siores E, Ball J, Blicblau A. Applications of fixed and variable frequency microwave (VFM) facilities in polymeric materials processing and joining. J Mater Process Technol 2001;113(1–3):184–8.

[265] Bows J. Variable frequency microwave heating of food. J Microw Power Electromagn Energy 1999;34(4):227–38.